Fundamental standards for acoustics based on optical methods – Phase three report for sound in water

Peter Theobald, Alex Thompson,
Stephen Robinson, Roy Preston,
Paul Lepper, Colin Swift,
Wang Yuebing and John Tyrer

January 2004

January 2004

FUNDAMENTAL STANDARDS FOR ACOUSTICS BASED ON OPTICAL METHODS – PHASE THREE REPORT FOR SOUND IN WATER

Peter Theobald[1], Alex Thompson[1], Stephen Robinson[1], Roy Preston[1], Paul Lepper[2], Colin Swift[3], Wang Yuebing[4] and John Tyrer[2]

[1]Centre for Acoustics and Ionising Radiation, National Physical Laboratory, Teddington, Middlesex TW11 0LW
[2] Department of Mechanical Engineering, Loughborough University, Ashby Road, Loughborough, Leicestershire LE11 3TU
[3]Laser Optical Engineering Ltd, PO Box 6321, Loughborough, Leicestershire LE11 3XZ
[4]Hangzhou Applied Acoustics Research Institute, 80 Guihuaxi Road, Hangzhou, Zhejiang, 311400, CHINA

ABSTRACT

This report documents the progress of work towards the development of fundamental standards for acoustics based on optical methods for sound in water between 1 kHz and 500 kHz. The favoured approach for achieving this is particle velocity measurement using heterodyne interferometry and a reflecting membrane in the acoustic field. This report focuses on investigations into a suitable design of reflecting membrane and the performance of the 'all-fibre' heterodyne interferometer. Some new developments on the new 'all-fibre' heterodyne interferometer are also reported together with the recent comparison results with a reference hydrophone calibrated using the reciprocity method. The report also presents some different optical techniques that can be employed for the transducer characterisation and mapping of acoustic fields.

This report is the Deliverable for the Phase Three Work Package for Project 3.6 of the NMS Quantum Metrology Programme for the UK Department of Trade and Industry. The sound in water aspect of the project is being undertaken by a consortium of the National Physical Laboratory and Loughborough University, with Laser Optical Engineering Ltd. as a sub-contractor.

ISSN 1740-0953

National Physical Laboratory
Queens Road, Teddington, Middlesex, UK, TW11 0LW

Approved on behalf of the Managing Director, NPL
by Dr R C Preston, authorised by Head of
Centre for Acoustics and Ionising Radiation

CONTENTS

1 INTRODUCTION

1.1 Project details

This project aims to lay the foundation for a new generation of primary acoustical measurement standards based on optical techniques for both sound in air and sound in water. The project entitled 'Fundamental standards for acoustics based on optical methods' is Project 3.6 of the National Measurement System (NMS) Quantum Metrology Programme of the UK Department of Trade and Industry. The project is being undertaken by a consortium of the National Physical Laboratory (NPL), Loughborough University (LU), Edinburgh University (EU), with Laser Optical Engineering Ltd. (LOE) and QinetiQ as sub-contractors. This report details progress on Phase Three of the project and addresses only the sound in water aspect of the project for which the project team consists of NPL, LU and LOE.

The first sixteen months of the project work was reported in the first and second stage reports [1] and [2] respectively, which included a comprehensive review of the literature, detailed the requirements for new sound in water standards, the reasons for using optical methods, the proposed use of a reflecting membrane in the acoustic field and the development of an all-fibre heterodyne interferometer essential to the proposed method.

1.2 Background

1.2.1 Reflective membranes in acoustic fields

Reflective membranes have been used for the optical measurement of acoustic fields for several years [3] [4] [5] [6] and form the basis of the NPL's primary standard for underwater measurement above 500 kHz [7] [8] [9]. For these higher frequency measurements a circular reflective membrane (pellicle) is stretched over a supporting ring with a 100 mm diameter. The diameter of the ring determines the lower frequency limit of the measurement due to acoustic reflections from this supporting ring. Below this limit, the homodyne interferometer used as the primary standard will have a lower frequency limit due to vibrational tolerances. This Quantum Metrology project has sought to address these two limitations by the development of a pellicle design suitable for measurement down to 1 kHz and development of an optical device optimised for the specific measurement requirements. A strip pellicle design has proven to be the most suitable for low frequency measurement and is discussed further in Chapter 2. The development of the optical device also had to consider other demanding design and operational criteria which were covered in the Phase Two report [2]. Chapter 3 also details some recent developments on the 'all-fibre' heterodyne interferometer and presents the results of a comparison with a reference hydrophone calibrated using the existing reciprocity method.

1.2.2 Methods for mapping of acoustic fields

Different techniques can be used for the mapping of two-dimensional and three-dimensional acoustic fields. This project has employed two methods that allow detailed maps of the acoustic field to be reconstructed.

The first of these employs a scanning vibrometer method for measuring the surface velocity of either the face of a transducer or a pellicle at a set distance from the transducer. The ability to scan the optical beam enables high-resolution two-dimensional maps of the near field to be obtained. The use of a pellicle at set distances would enable one to extend this re-construction to a limited resolution three-dimensional map of the near field.

The second technique exploits the acousto-optic effect produced when an acoustic wave passes through a volume of fluid. The resultant change of density and thus refractive index can be detected by an interferometer or vibrometer. The change in refractive index can also cause lateral shifts of the beam which may have a significant effect where using a phase type interferometer. This would be less important for a vibrometer responding to a Doppler shift. The use of a scanning measurement system allows pressure maps of the acoustic field to be reconstructed from a finite number of line integrals across the acoustic beam. The technique is literally non-intrusive and can therefore be used to measure fields where a hydrophone or even a pellicle would not be suitable. The measurement of lithotripter fields is such an example, where conventional hydrophones can be destroyed by the shock wave.

1.3 Outline of report

The structure of the report is as follows. Chapter 2 describes the rationale for the pellicle design and presents experimental data demonstrating its performance over the required frequency range. Chapter 3 details recent developments of the ‘all-fibre’ heterodyne interferometer and presents results characterising its performance over an extended frequency and dynamic range. This also includes a comparison with a reference hydrophone. Chapter 4 introduces optical scanning techniques for the near-field evaluation of acoustic fields. Optical transducer scans are compared with conventional hydrophone scans. Chapter 5 discusses the work being undertaken on the study of acousto-optic techniques for the mapping of acoustic fields. This work includes measurements of high intensity focussed ultrasonic fields. The final chapter summarises the work undertaken in Phase Three of the project and discusses improvements necessary to deliver Phase Four successfully.

2 PELLICE FOR 1 kHz TO 500 kHz ACOUSTIC MEASUREMENT

2.1 Introduction

A thin membrane that closely matches the acoustic impedance of water will follow the particle displacement of the acoustic wave with negligible deviation [5]. The use of such a pellicle allows for an optically reflective boundary layer to be introduced into the measuring medium which will allow the particle displacement or velocity to be measured optically without perturbing the acoustic field.

2.2 Pellicle design

The ring type pellicle used as part of the primary standard for hydrophone calibration above 500 kHz is not suited to lower frequency measurement due to acoustic reflections from the supporting ring and the impracticalities of making a very large support ring. To overcome this, the proposed method uses a strip type pellicle, such that the supporting structure provides a sufficient reflection-free window to measure down to a few kilohertz.

Figure 1 shows the design of the pellicle frame used for the measurements presented in this report. The square frame was manufactured from 33 mm square extruded aluminium beams, 1.3 m in length, with strengthening side supports to increase torsional rigidity. A mounted pole at the top of the frame allowed mating with the micro positioning system on the NPL small open water tank. A 1.3 m membrane or pellicle of the desired width was then tensioned between the top and bottom of the frame.

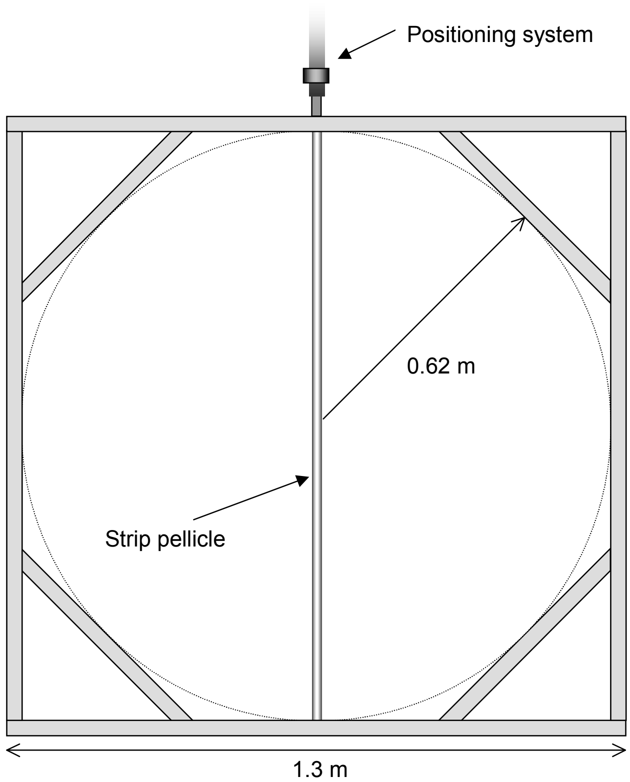

Figure 1. Schematic of support frame for strip pellicle.

When used with a projector separation of 0.5 m, this 1.3 m frame/pellicle combination should provide a reflection free measurement time window of around 0.62 ms following the initial arrival from the projector.

2.3 Initial measurements using strip pellicle

Measurements were performed in the NPL small test tank using a strip type pellicle and a Polytec CLV-1000 vibrometer with a CLV-700 optical head. The measurements were performed to test the suitability of the strip pellicle design and the supporting frame.

2.3.1 Measurement procedure

The vibrometer was positioned using a camera tripod such that the laser beam entered the test tank (2 m x 1.5 m x 1.5 m) through the access window shown in Figure 2a. The optical beam was first positioned on the acoustic centre of the acoustic projector; the pellicle was then inserted in the path of the optical beam such that the projector to pellicle separation was 0.5 m. The beam was then reflected from the pellicle, returning to the collection lens on the vibrometer head, with the electrical signal output of the vibrometer digitised using a HP89410A vector signal analyser. The laser beam was oriented such that the beam was “head on” to the acoustic wave front.

Several membranes of different thickness and width were used during the measurements which were all 1.3 m in length and tensioned over the 1.3 m pellicle frame shown in Figure 1. Attachment of the frame to the positioning system on the small NPL tank allowed rotational adjustment of the pellicle to obtain a maximum signal return. This arrangement is shown in Figure 2b.

The membranes used were, a 12.6 mm wide cassette tape with a thickness of 25 µm, a 4.6 mm wide cassette tape with a thickness of 17 µm and a 10 mm strip of Mylar with a thickness of 23 µm coated on one side with 40 nm of aluminium. It is important to note that the cassette tapes were not coated and therefore produce a defuse reflection. Care was taken in each case to ensure that the return light level indicator on the Polytec vibrometer indicated an optimum return.

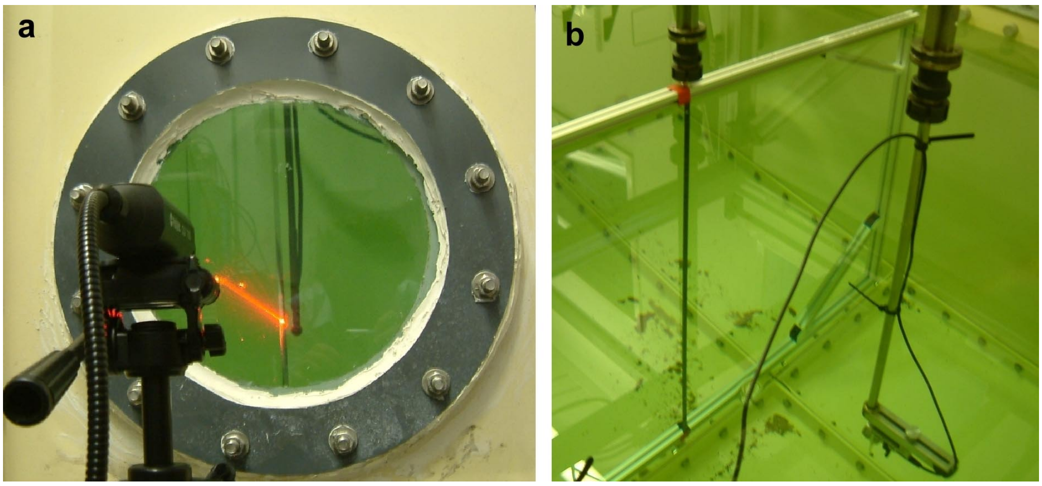

Figure 2. a) Photograph of the optical beam reflecting off the pellicle. b) Photograph of pellicle support frame in the NPL small tank with an acoustic projector.

Four transducers were used as acoustic sources for a series of measurements:

- ITC1001 – a 150 mm diameter sphere with a resonance at 18 kHz, used for the range 2 kHz to 40 kHz.
- ITC1042 – a 25 mm diameter sphere with a resonance at 75 kHz, used in the range 7 kHz to 200 kHz.
- Reson TC4023/33 – a 25 mm diameter sphere with a resonance at 90 kHz, used for the ranged 100 kHz to 250 kHz.
- Panametrics piston – 1.5" diameter piston transducer with a resonance of 0.5 MHz, used for the range 100 kHz to 300 kHz.

The acoustic projectors were driven with time-gated tone-bursts of 0.45 ms in length and signal amplitudes between 50 and 150 $V_{p\text{-}p}$, by a HP-331020A function generator coupled to a B&K 2713 40 dB power amplifier. The captured signal was time windowed to isolate the acoustic reflections such that measurements were only made on the steady-state portion of the direct path signal. In each case, an NPL reference hydrophone was used to provide an independent measure of the acoustic output of the source. At lower frequencies, a B&K8100 hydrophone was used, and a Reson TC4034 was used to cover an extended frequency range. These had previously been calibrated using the reciprocity method.

The measurement procedure consisted of positioning the projector 0.5 m from the rear of the tank and aligning the laser beam so that it was positioned on the acoustic axis of the acoustic projector such that the optical and acoustic beams were co-linear. The pellicle was then positioned in the path of the optical beam, 0.5 m from the projector. Small adjustments were made to the lateral (horizontal) position and orientation of the pellicle to ensure maximum light return to the vibrometer. Measurements were made of the steady-state acoustic velocity at a range of frequencies using the vibrometer. The hydrophone was then positioned in the acoustic field such that the optical beam was incident on the acoustic centre of the hydrophone. The steady-state acoustic velocity was then calculated from the measurements of acoustic pressure made with the reference hydrophones (the calculations were performed using the plane-wave relationship between acoustic pressure and acoustic particle velocity) for the same frequencies. A comparison was then possible between the acoustic velocity measured using the optical method and that obtained from the reference hydrophone. The sensitivity of the reference hydrophone was also calculated using the optical measurement data and compared to the reference reciprocity data for the same hydrophone. This procedure was repeated several times using different acoustic projectors and hydrophones to cover an extended frequency range. Measurements were also repeated using different pellicle arrangements.

Measurements were further made using the vector signal analyser of the noise spectra obtained from the output of the vibrometer without the acoustic signal present.

2.3.2 Vibrometer characterisation

The vibrometer used throughout the measurements was a Polytec CLV-1000 vibrometer with a CLV-700 optical head. The modules fitted in the CLV-1000 allowed a pre-filter output with 3 dynamic range settings: 2 mm/s/V, 10 mm/s/V and 50 mm/s/V. A second output allowed the use of a filter unit which consisted of both high-pass and low-pass units. All acoustic measurements were performed using the 2 mm/s/V sensitivity setting and the full bandwidth output at the pre-filter stage. Figure 3 shows the noise floor performance of the vibrometer at each of its sensitivity settings and also with the use of the built in 100 kHz LP filter. The noise floor measurements were performed for a reflection from the 12.6 mm cassette tape.

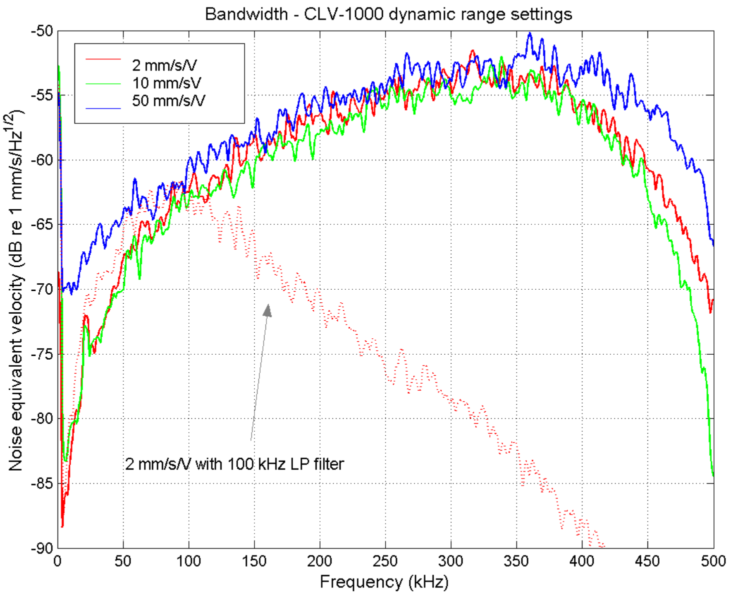

Figure 3. Noise equivalent velocity of Polytec vibrometer showing bandwidth of each sensitivity setting.

2.3.3 Analysis of results

Figure 4 shows examples of some digitised time waveforms captured from the signal output of the vibrometer using the 12.6 mm wide pellicle. In this case, the ITC 1042 was used as the projector and the signals were captured using 32 onboard time averages with the HP vector signal analyser. These show a good representation of the acoustic signal, where the start and end components of the tone-burst are affected by the projector resonance.

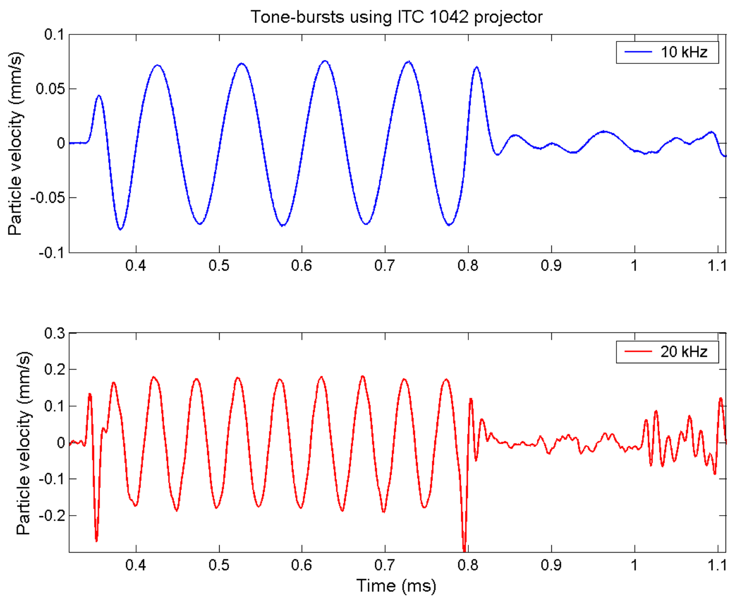

Figure 4. Particle velocity measured from the 12.6 mm wide pellicle using the Polytec vibrometer.

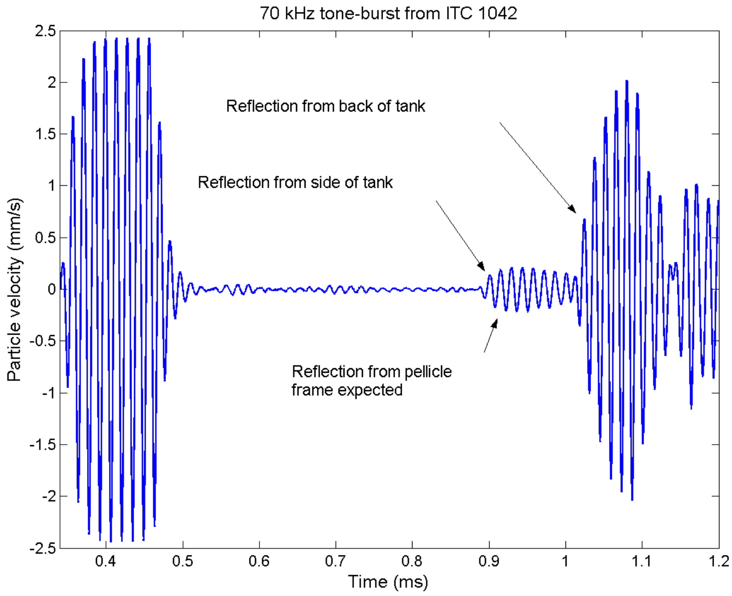

Figure 5. High frequency tone-burst showing reflections from the pellicle frame and the tank (the main received signal is shown on the left).

With the measurement arrangement used, the echo-free time following the direct wave arrival at the receiver position in the small test tank was just less than 0.6 ms. The reflections highlighted in Figure 5 occur in the first instance from the side of the tank, where small reflections were expected from the pellicle support frame at around the same time. The measurement plane was slightly off centre from the long axis of the tank, so the first reflection was from a single side of the tank, followed closely by the reflection from the opposite side and from the back wall of the tank, 0.5 m behind the projector.

2.3.3.1 Velocity measurements using 12.6 mm wide tape pellicle

Measurements performed using the 12.6 mm wide tape pellicle covered the frequency range 7 kHz to 300 kHz in two ranges. The first range used an ITC1042 (120 V_{p-p} drive level) as the projector between 7 kHz and 200 kHz. The second frequency range between 100 kHz and 300 kHz used a Panametrics 0.5 MHz piston transducer (120 V_{p-p} drive level) as the projector. Each frequency range comprised two acoustic velocity datasets; one measured using the optical method and the second measured using the Reson TC 4034 reference hydrophone. The hydrophone measurements were performed using the Reson VP1000 pre-amplifier set with a nominal gain of 20 dB. A Krohn-Hite 3944 band-pass filter unit was used on the output of both the vibrometer and the hydrophone, using a band-pass of one octave either side of the drive frequency.

The sensitivity was also calculated for the reference hydrophone using the optical comparison method. In each case this was plotted against the reference hydrophone reciprocity calibration data, where the uncertainty of the reciprocity data is ±0.5 dB for a 95% confidence level. The pressure sensitivity plots represent ‘calibration data’ for which an example is shown in Figure 6b, where Figure 6a is the velocity data measured directly using the optical method and calculated using the reciprocity data for the reference hydrophone.

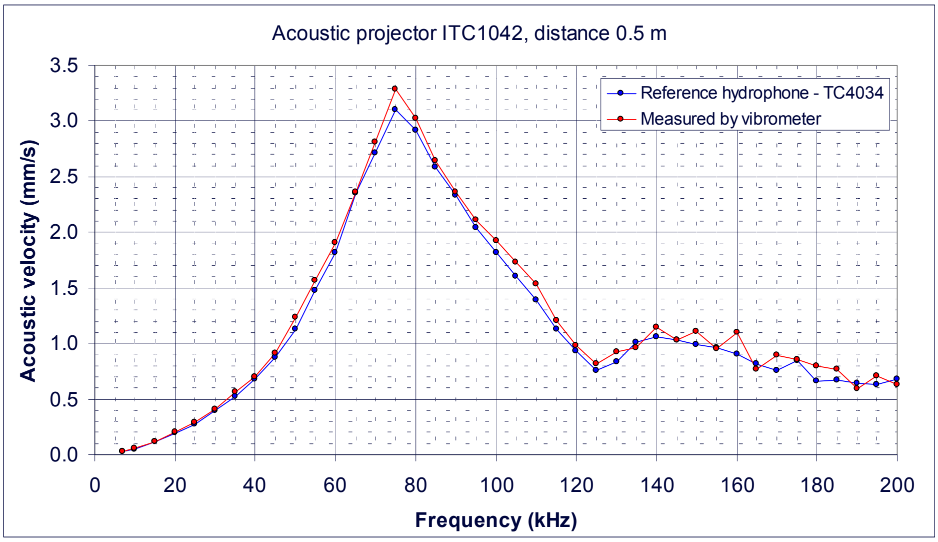

Figure 6a. Acoustic velocity measurements using reference hydrophone and vibrometer with a sensitivity setting of 2 mm/s/V.

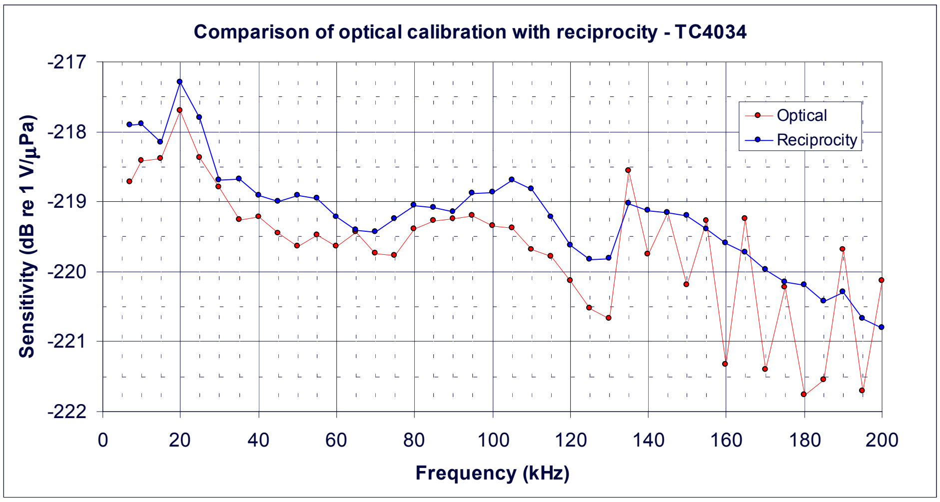

Figure 6b. Calibration data using reciprocity and optical comparison with a vibrometer sensitivity setting of 2 mm/s/V.

Figure 7 shows the same measurements as Figure 6 performed with a lower sensitivity setting (10 mm/s/V) on the vibrometer. Figure 3 showed that the noise floor level of the 2 mm/s/V and the 10 mm/s/V sensitivity settings were very similar. For all other measurements presented in this report, unless stated otherwise, a vibrometer sensitivity setting of 2 mm/s/V was used.

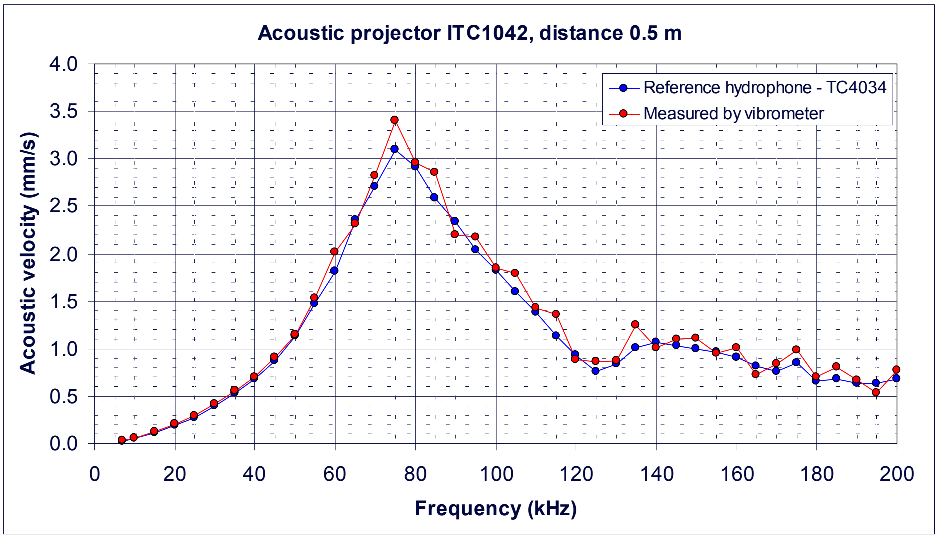

Figure 7a. Acoustic velocity measurements using reference hydrophone and vibrometer with a sensitivity setting of 10 mm/s/V.

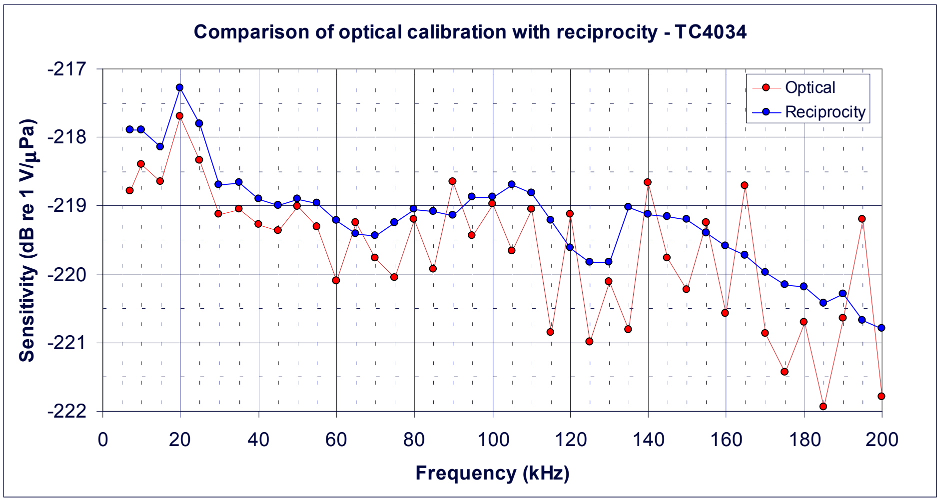

Figure 7b. Calibration data using reciprocity and optical comparison with a vibrometer sensitivity setting of 10 mm/s/V.

Figures 8a and 8b are the results obtained for an extended frequency range up to 300 kHz using the Panametrics 0.5 MHz piston projector (120 $V_{p\text{-}p}$ drive level). It should be noted that the 300 kHz data point in Figure 8a was obtained at a reduced drive level of 80 $V_{p\text{-}p}$.

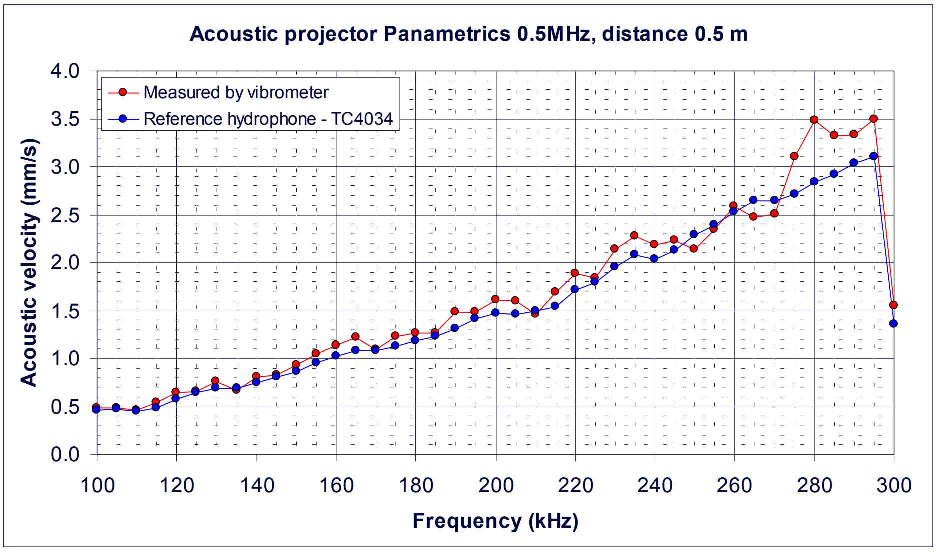

Figure 8a. Acoustic velocity measurements using reference hydrophone and vibrometer.

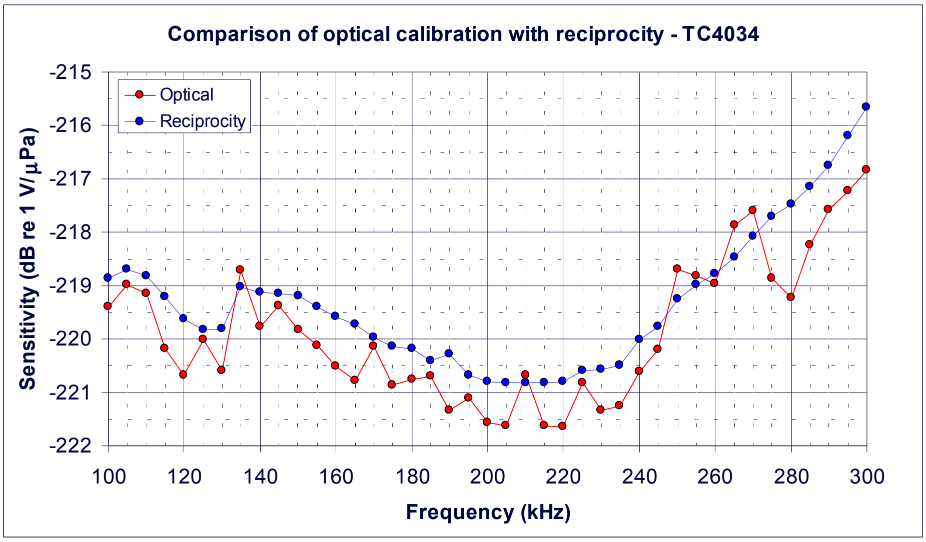

Figure 8b. Calibration data using reciprocity and optical comparison with the vibrometer.

The results obtained in the first batch of measurements using the 12.6 mm strip pellicle showed two points of interest:

1. The sensitivities obtained using the optical method exhibited a consistent lower sensitivity (or higher velocity) across the frequency range used. The gain of the Reson VP1000 pre-amplifier was assumed to be its nominal value of 20 dB in the calculation of the velocity and the sensitivity (the pre-amplifier gain must be subtracted from the overall output). The gain of the amplifier was measured over a range of frequencies and was found to be 19.5 dB throughout most of its operating range with a roll off at low frequencies. For subsequent measurements, which are shown in Figure 9 and onwards, corrections were applied using values of he measured amplifier gain. This significantly improved the agreement between the two methods.

2. There were amplitude fluctuations with frequency. This was particularly evident at higher frequencies where the response of the optical measurement was clearly in disagreement with the hydrophone measurements. It was thought that this could have

been caused by vibration modes across the width of the pellicle. For the 12.6 mm pellicle, one might expect the fundamental flexural mode at around 60 kHz. This was evident in Figure 7b, although Figure 6b and 8b indicated no evidence of flexural modes until around 120-130 kHz. The drive levels used in each case were similar, with the set-up used to obtain Figure 6b and 7b being identical except for the different sensitivity setting on the Polytec vibrometer. The measurements to obtain Figure 7 were performed directly following the measurements performed to obtain Figure 6 with no other changes to the experimental setup. The discrepancy is therefore surprising and unknown at this stage.

The amplitude fluctuations in the frequency domain were also observed during initial measurements reported in Phase One of the project [1] [11]. During these measurements a wider strip pellicle was used with a width of 20 mm. The amplitude artefacts in this case were evident between around 5 kHz and 30 kHz and were assumed at the time to be caused by reflections present in the windowed signal. It is now thought that this discrepancy was also caused by flexural modes in the pellicle.

2.3.3.2 Velocity measurements using 4.6 mm wide tape pellicle

The second batch of measurements were performed using a narrower pellicle. If in fact the amplitude fluctuations in the frequency domain were due to flexural modes in the membrane, then one would expect the frequency of the onset of the amplitude fluctuations to be inversely related to the pellicle width. This was indeed the case and allowed for an increased measurement frequency range. The membrane used in this case was the 4.6 mm wide cassette film, which was also thinner than the 12.6 mm pellicle. The membrane was sufficiently thin that it allowed noticeable light transmission.

Measurements performed using the narrow pellicle covered the same frequency range as those performed using the 12.6 mm pellicle, 7 kHz to 300 kHz in two ranges, to allow a direct comparison. The hydrophone measurements in this case were also corrected for the measured pre-amplifier gain. These results are shown in Figures 9-10. Where the ITC1042 (120 V_{p-p} drive level) projector was used between 7 kHz and 200 kHz and the Panametrics 0.5 MHz piston transducer (120 V_{p-p} drive level) was used between 100 kHz and 300 kHz. The hydrophone measurements were performed using the Reson VP1000 pre-amplifier set with a nominal gain of 20 dB. The Krohn-Hite band-pass filter was set to 1 octave and was used for both the hydrophone and vibrometer measurements.

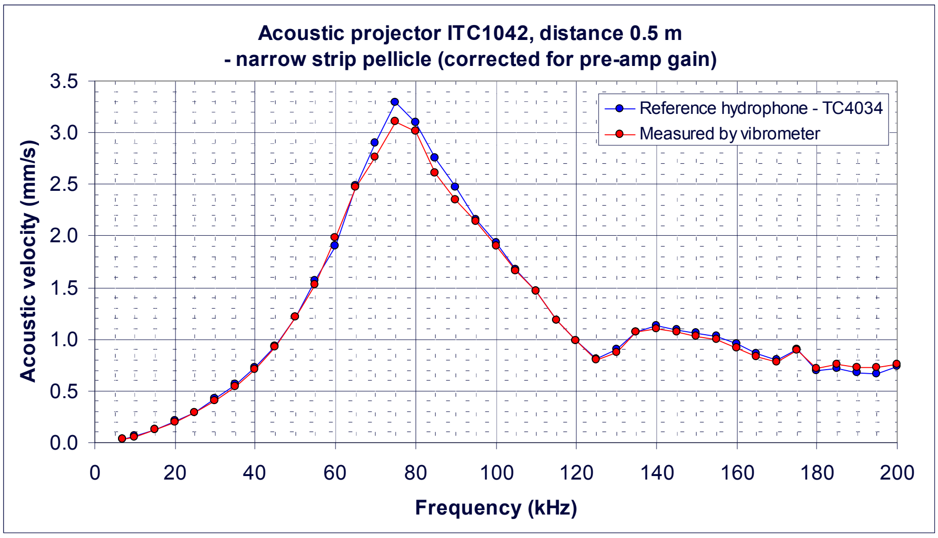

Figure 9a. Acoustic velocity measurements using reference hydrophone and vibrometer.

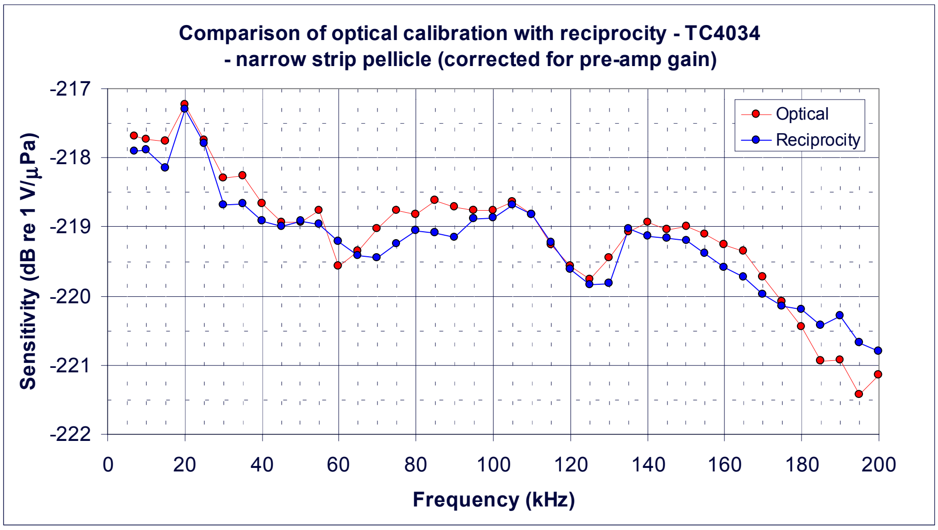

Figure 9b. Calibration data using reciprocity (±0.5 dB for 95% confidence level) and optical comparison with the vibrometer.

Using the 4.6 mm wide pellicle removed the effect of flexural modes across the width of the membrane up to around 300 kHz where they were clearly evident with the 12.6 mm wide pellicle. This can be seen by comparing Figure 9b with Figure 6b which were identical measurements except for the different pellicles used. Although the agreement between the optical method and the reference hydrophone using the 4.6 mm pellicle was better than that with the 12.6 mm wide pellicle, the optical technique still showed a velocity somewhat less than that determined using the hydrophone around the resonance of the projector. Overall, agreement between the optical calibration results and the reciprocity data was better than 0.5 dB between 7 kHz and 200 kHz. This agreement is excellent considering the calibration uncertainty in the reference data is ±0.5 dB for a 95% confidence level.

Using the Panametrics projector (see Figure 10) the greatest disagreement occurred around 200 kHz where the difference in sensitivity between the optical method and the reciprocity data was as much as 1 dB. The reasons for this are explored further towards the end of this sub-section.

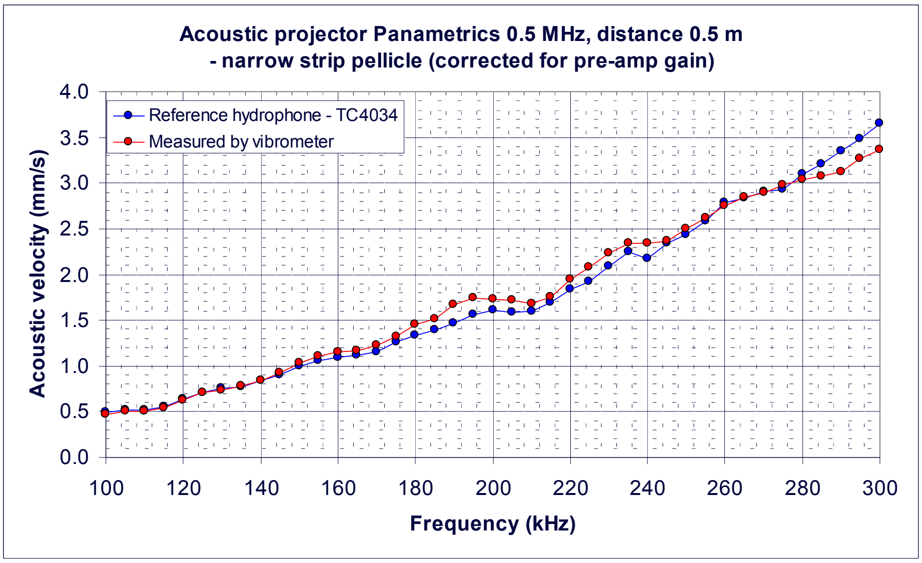

Figure 10a. Acoustic velocity measurements using reference hydrophone and vibrometer with a Panametrics 500 kHz piston projector.

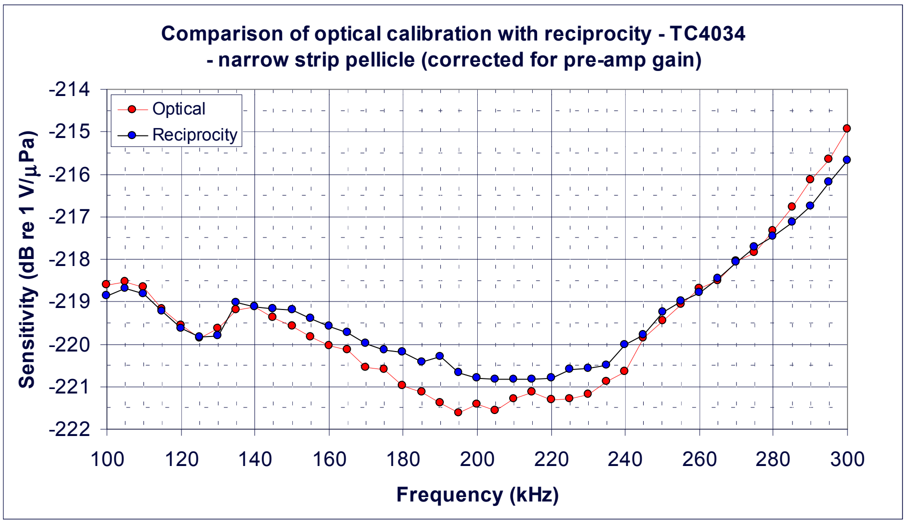

Figure 10b. Calibration data using reciprocity and optical comparison with a Panametrics 500 kHz piston projector.

In addition to these repeat measurements with the 4.6 mm pellicle, measurements were performed using the ITC1001 acoustic projector (150 $V_{p\text{-}p}$ drive level) in the range 2 kHz to 40 kHz (see Figure 11 and 12) and the Reson TC4023 projector (80 $V_{p\text{-}p}$ drive level) in the range 140 kHz to 250 kHz (see Figure 13). When performing the hydrophone measurements (with the Reson TC4034) for the Reson TC4023 projector, the Reson VP1000 hydrophone pre-amplifier gain was set to 6 dB, which was actually measured to be 5.6 dB. A 1 octave band-pass filter was still used. A 20 dB pre-amplifier gain was used for the measurements of the ITC1001 projector.

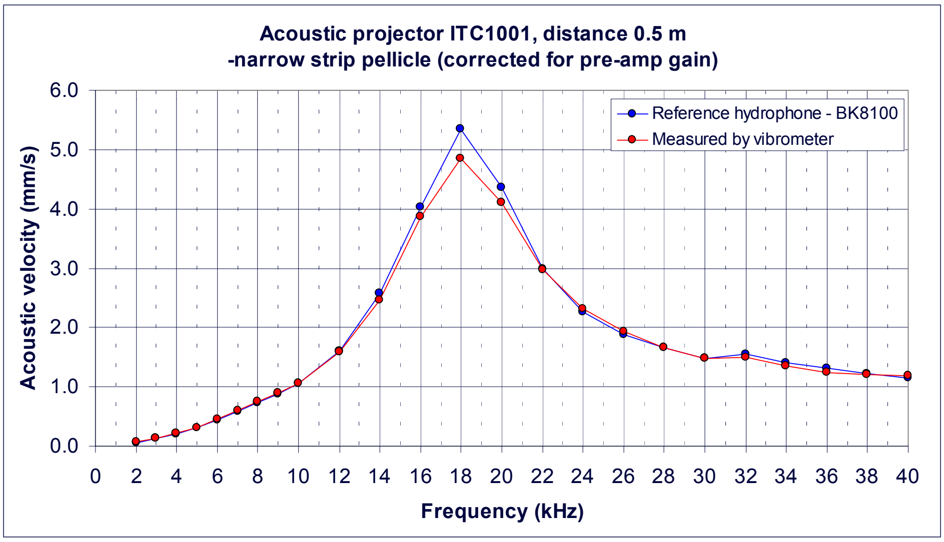

Figure 11a. Low frequency acoustic velocity measurements using reference hydrophone and vibrometer with an ITC1001 projector.

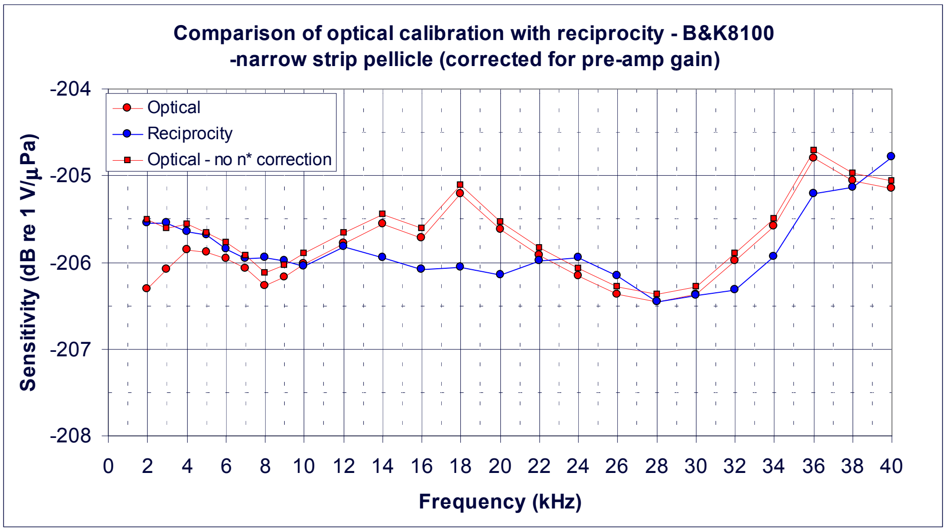

Figure 11b. Low frequency calibration data using reciprocity and optical comparison with the vibrometer with an ITC1001 – corrected and uncorrected for the effective refractive index n*.

Generally, the agreement using the ITC1001 at lower frequencies was very good, in most cases better than 0.5 dB down to 4 kHz. However, accurate measurements below 5 kHz could not be expected in the small NPL tank due to the limited reflection free time window. The disagreement at 18 kHz coincides with the resonance of the projector and so was thought to be caused by an excessive projector drive level (see Figures 11a and 11b). Repeat measurements were performed with a lower drive level (80 V_{p-p}) which are shown in Figures 12a and 12b. The measured acoustic velocity using the lower drive level was around half that shown in Figure 11a and the agreement around the resonance was much improved. Figure 11a, at the high drive level, showed a disagreement of nearly 1 dB whereas Figure 12b using the lower drive level resulted in an agreement of better than 0.5 dB.

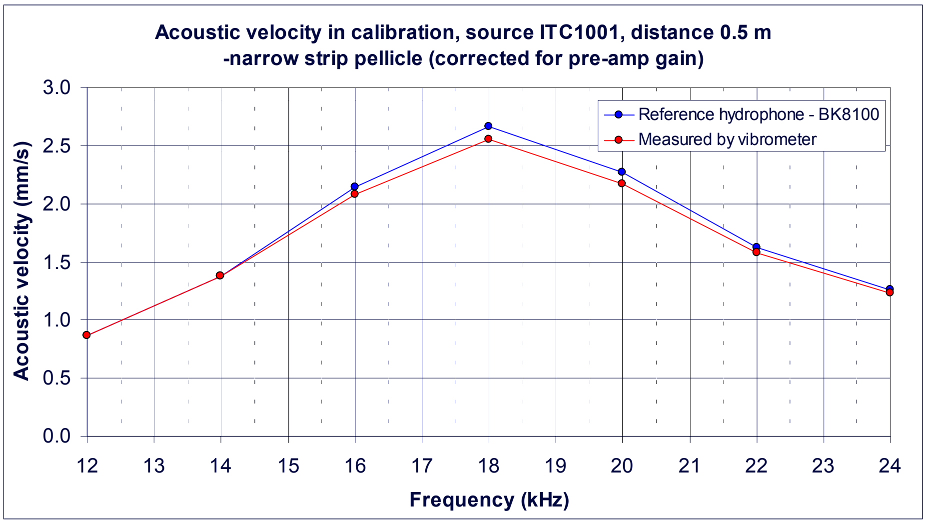

Figure 12a. Low frequency acoustic velocity measurements using reference hydrophone and vibrometer (ITC1001 reduced drive level).

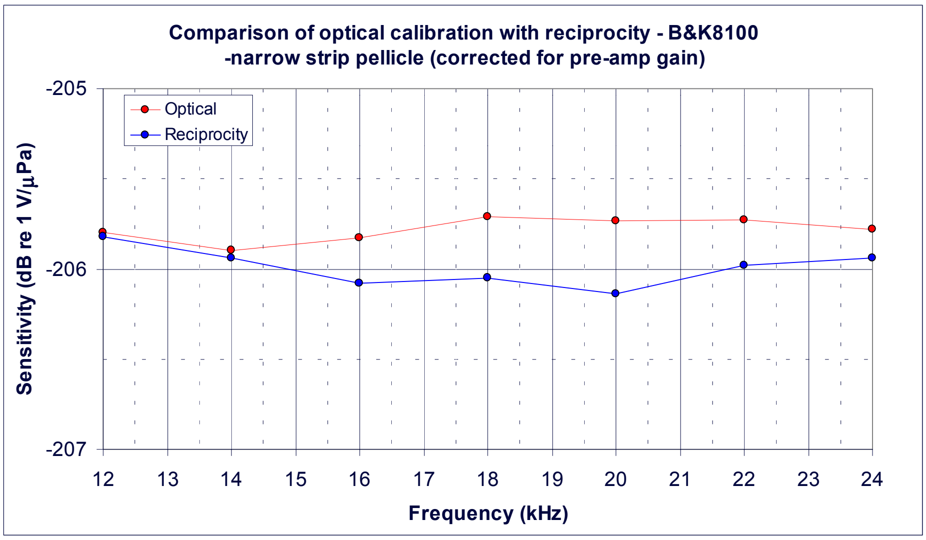

Figure 12b. Low frequency calibration data using reciprocity and optical comparison with the vibrometer (ITC1001 reduced drive level).

The results shown in Figures 11 were also corrected for the acousto-optic effect as the effective refractive index, n*, begins to deviate from unity (actually 1.01) below about 18 kHz. Figure 11b also shows the uncorrected data on the same plot as that corrected for the effective refractive index, n*. The data used for the effective refractive index is shown in Table 1, obtained using a spherical wave correction derived in the Phase Two report [2] for the specific measurement geometry used. The results shown with no correction for n* exhibit better agreement with reciprocity than the optical results that have been corrected for n*. The correction was applied as a simple factor to the velocity. At around 20 kHz and above, the correction factor would be 1.01. It is unclear at this stage if the correction factor should be applied as an 'effective refractive index' as the vibrometer is not reliant on the refractive index of the material to derive its absolute velocity.

For the higher frequency applications at NPL, a Michelson displacement interferometer is used where the change in refractive index causes an apparent offset in path length of the optical beam. Importantly for this application, the change in refractive index over a number of traversed acoustic cycles is a constant offset from the standard refractive index of water. The vibometer, used in its velocity mode is therefore unaffected by this refractive index offset as the vibrometer is sensitive to a rate of change. This is a potential advantage using a vibrometer rather than a standard displacement interferometer. At lower frequencies where only a few acoustic cycles occur in the optical propagation distance the density and therefore the refractive index will not be constant and the vibrometer will potentially respond to a small rate of change in the medium.

For other applications, such as acousto-optic field mapping where the change in refractive index is exploited to detect the acoustic field, the vibrometer will be very sensitive to the rate of change of the refractive index as the beam crosses the acoustic beam.

Table 1. Effective refractive index data.

Frequency (kHz)	Effective refractive index, n*
2	1.095
3	1.056
4	1.035
5	1.027
6	1.022
7	1.018
8	1.017
9	1.015
10	1.015
12	1.014
14	1.013
16	1.013
18	1.012
20	1.010
22	1.010
24	1.010
26	1.010
28	1.010
30	1.010
32	1.010
34	1.010
36	1.010
38	1.010
40	1.010

The measurement data shown in figure 10b clearly shows a lower sensitivity dip at around 200 kHz using the Panametrics 500 kHz piston projector. The measurements performed to obtain Figure 10 where repeated for a similar frequency range using a Reson TC4023 ball projector in attempt to isolate the cause of the disagreement. The measurement results are shown in figures 13a and 13b. Although not so clearly defined, the optical method resulted in a sensitivity lower than the reciprocity data around 200 kHz. The reason for this consistent disagreement at 200 kHz was not clear although it was possibly due to a variation in the sensitivity of the vibrometer. The 2 mm/s/V sensitivity setting is a nominal value and could vary across the frequency range of the vibrometer. It is possible that vibrometer is slightly more sensitive around 200 kHz.

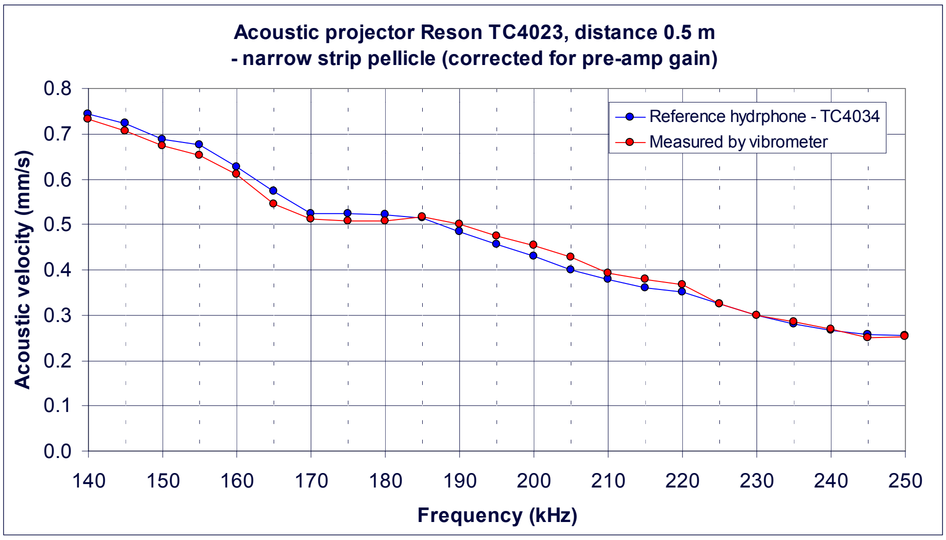

Figure 13a. Mid-frequency acoustic velocity measurements using reference hydrophone and vibrometer with a TC4023 projector.

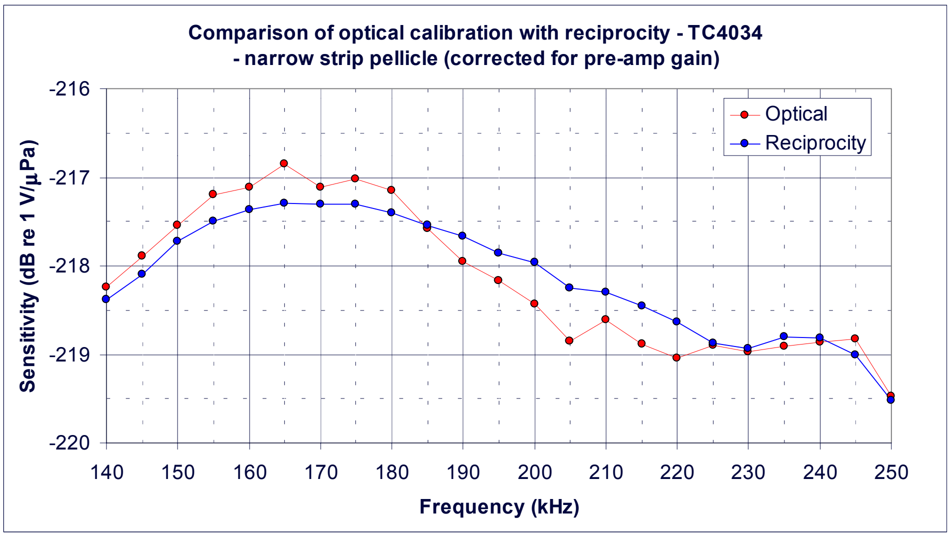

Figure 13b. Mid-frequency calibration data using reciprocity and optical comparison with the vibrometer with TC4023 projector.

2.3.3.3 Velocity measurements using 10 mm wide reflective Mylar pellicle

Generally, the signal-to-noise ratio using the two types of cassette tape was poor and the drive level to the projector was therefore increased such that the velocities being measured were of the order of several millimetres per second. The tape was used as it provided a good quality strip of uniform width and had been successfully used in the literature [10] for optical measurement techniques. The return light level indicator on the Polytec CLV-700 optical head indicated a maximum light return for optimum signal-to-noise ratio so the need for a reflective target was not initially considered when using the tape. However, changing to a reflective pellicle, cut into a 10 mm strip provided a significant improvement in signal-to-noise ratio such that velocities less than 1 mm/s were measured (see Figure 14a). Although the vibrometer indicated the same light return (maximum), the signal-to-noise ratio improved several times. The reason for this was thought to be that the cassette tape produced a diffuse (de-polarized) reflection, which could not be utilised fully by the vibrometer due to its use of polarising beam splitters to separate the returning light. In such a case, although a significant amount of light may return to the optical head, only a small fraction of it would be used to produce the interference signal on the photodiodes. A highly reflective surface would overcome this by maintaining the polarisation plane of the returning light. The design of the new all-fibre heterodyne vibrometer does not rely on polarising components and would therefore not be degraded by the use of a diffuse surface in the same way.

The results using the 10 mm reflective pellicle however, did not produce a good agreement with reciprocity. The flexural modes observed in previous measurements were more pronounced even at lower frequencies. It was thought that this might be caused by a non-uniform pellicle width. The Mylar was a similar thickness (23 μm) to the 12.6 mm wide cassette tape which was 25 μm thick. The Mylar also had a 40 nm coating which was thought to be too insignificant to affect the overall material properties of the pellicle.

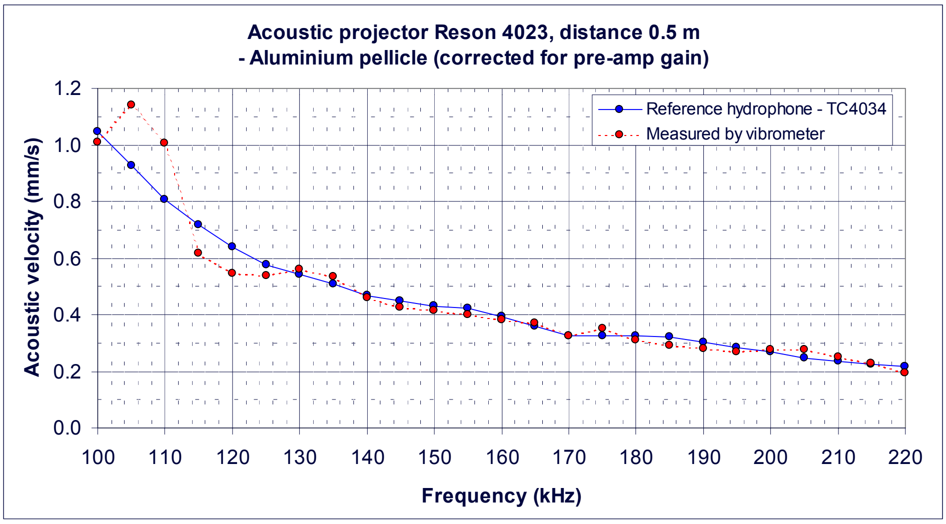

Figure 14a. Optical measurements using a 10 mm Mylar reflective pellicle compared with a reference hydrophone using a TC4032 projector.

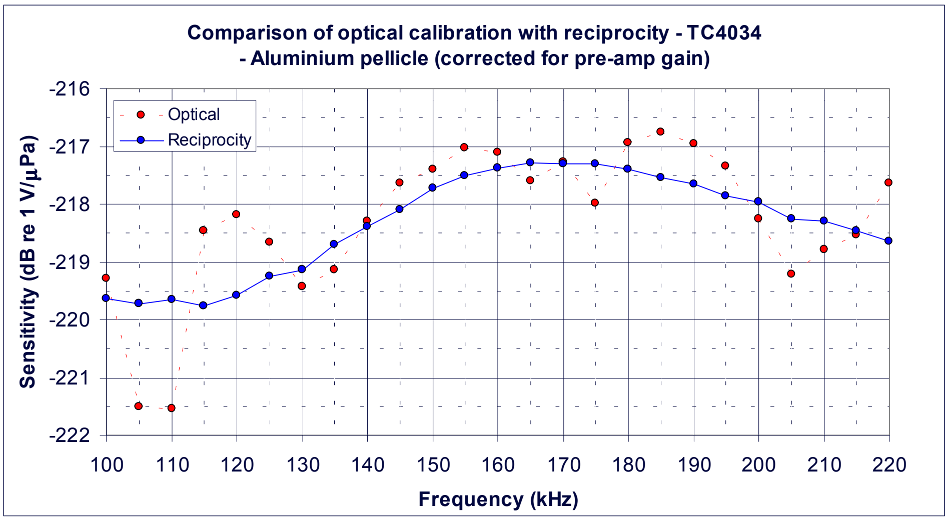

Figure 14b. Comparison of optical calibration of hydrophone using 10 mm Mylar reflective pellicle compared with reference reciprocity data for a TC4023 projector.

Further measurements are presented in sections 2.4 and 2.5 which investigate the pellicle modes and the use of narrower pellicles to reduce the effects of the pellicle modes.

2.4 Vibrometer scanning of pellicle modes

The presence of vibrational modes on the pellicle were first suggested in section 2.3.3.1 following observations of amplitude variations with frequency. The vibrational modes of concern are anti-symmetric with displacement normal to the width of the membrane. To investigate these further, a Polytec PSV 300 scanning vibrometer was used consisting of an OFV 056 scanning head and a PSV-Z-040-F control unit.

Three aluminium coated Mylar pellicles were scanned to investigate the flexural modes, widths being 3 mm, 5 mm and 10 mm. The scanning vibrometer was arranged to scan the surface of the pellicle through the glass window of the small NPL tank, with the 1.3 m square pellicle frame positioned in the centre of the tank and the projector positioned at a stand-off distance of 0.23 m and then 0.5 m. The projector used was a Panametrics 0.5 MHz piston transducer excited with tone-bursts at a number of frequencies between 100 kHz and 500 kHz. Scans were then performed over a rectangular area of the pellicle surface centred on the acoustic axis of the projector. Scan areas were approximately the width of the pellicle by a few centimetres in height, with the number of scan points totalling 610 points for the 3 mm pellicle, 854 points for the 5 mm pellicle and 1342 points for the 10 mm pellicle. A two-dimensional image obtained from the scan of the 5 mm pellicle is shown in a Figure 15, with a velocity line profile shown in Figure 16. Figure 17 shows a three-dimensional plot of the same pellicle at its maximum negative velocity position. Figures 15, 16 and 17 all show the pellicle behaviour in a 220 kHz acoustic field.

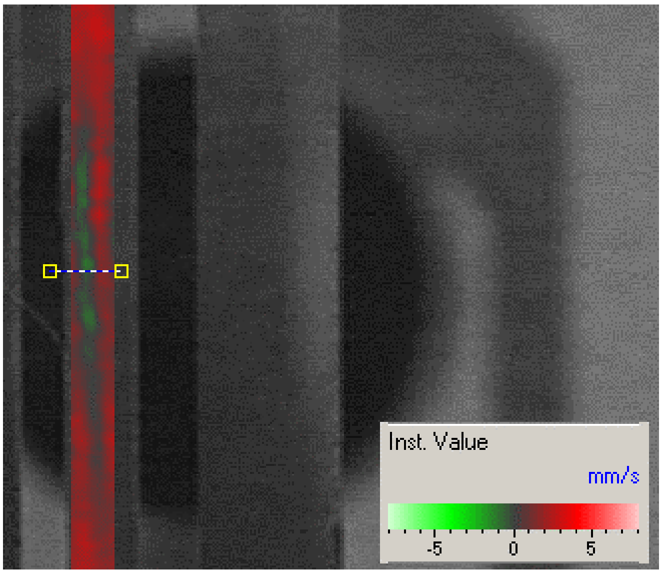

Figure 15. Two-dimensional plot showing the velocity scan of the 5 mm pellicle at its zero velocity point.

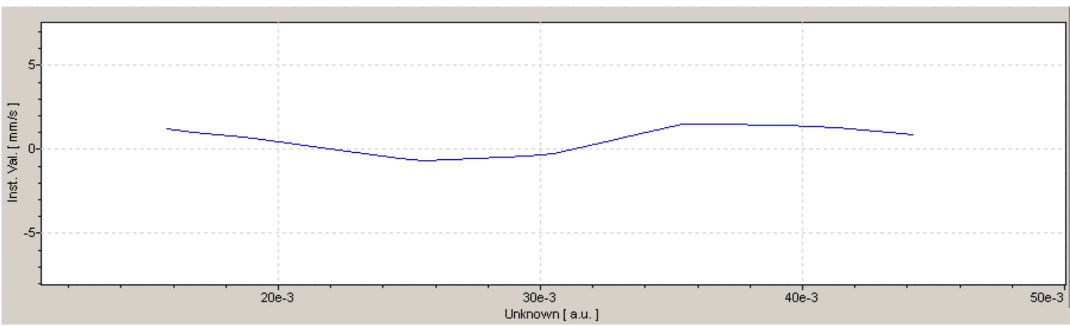

Figure 16. Line profile of 5 mm pellicle shown in Figure 15 (between the ‘index’ marks).

The image in Figure 15 shows the vibrometer camera image used for mapping out the scan area, with the scan data overlaid on the camera image. The Panametics projector can be seen in the background with the 3 mm and 10 mm pellicles either side of the 5 mm, each of which were each moved into position for their respective scans. The apparent lateral offset of the two-dimensional velocity map was caused by the differing lateral positions of the camera lens and the laser lens. In practice, the scan area was positioned centrally on the pellicle. The x-axis in Figure 16 shows arbitrary units, which refer to an angular reference used by the vibrometer during the scan. The absolute scale of the x-axis therefore depends on the number of scan points selected, the overall scan area and the vibrometer stand-off distance. The overall width of the scan shown in Figure 15, 16 and 17 was around 4 mm centred on 5 mm width of the pellicle. This provided a horizontal scan resolution of around 0.5 mm.

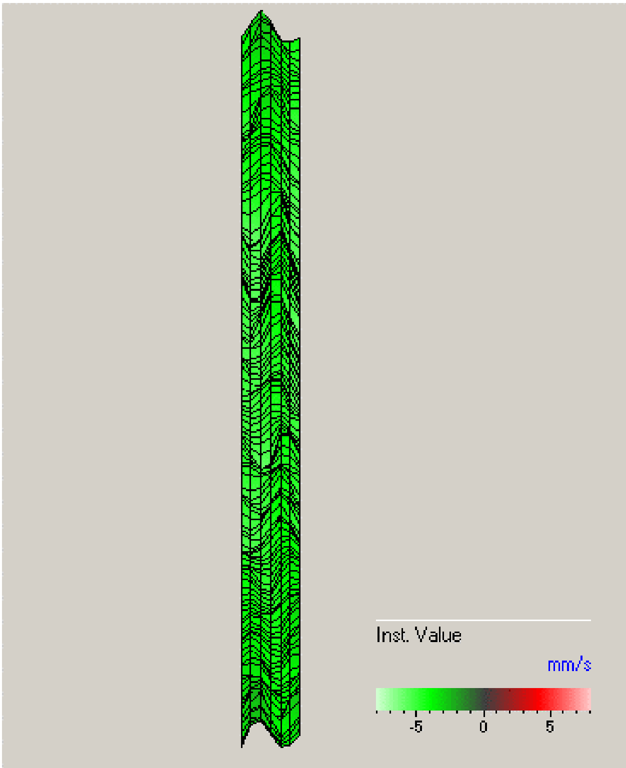

Figure 17. Three-dimensional plot of 5mm pellicle scan for a maximum negative velocity.

The scans clearly showed the non-uniform nature of the pellicle across its width, which was shown in Figures 15, 16 and 17. These modes appeared to have a dependence on pellicle width which was evident when comparing the scans from the 3, 5 and 10 mm pellicles (see Figure 18 for the 100 kHz example).

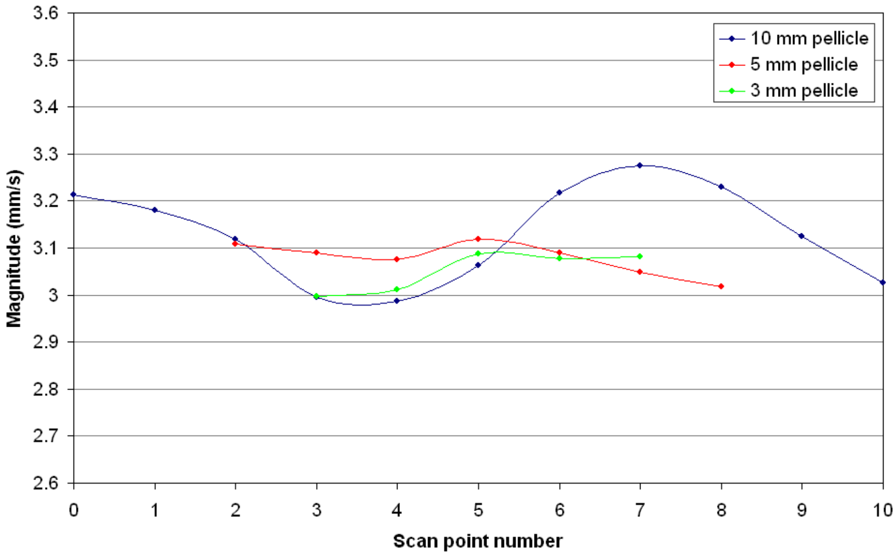

Figure18. Velocity magnitude scans across width of 3 different pellicles at 100 kHz.

In general, the scans showed a trend for a narrower pellicle to shift the on-set of the modes up in frequency and decrease the non-uniform behaviour at lower frequencies. Figure 18 shows that the 10 mm pellicle was affected much more at 100 kHz than the 5 mm or the 3 mm pellicles. The 3 mm and the 5 mm pellicles did exhibit some non-uniform behaviour at 100 kHz which one might not expect, particularly at 3 mm. It was thought that a non-uniform tension applied to the supporting ends of the pellicle, and a non-uniform width might have contributed to a non-uniform profile of the pellicle as it followed the acoustic field.

Figure 19 shows the effect of increasing frequency on the 5 mm pellicle. At 100 kHz, the magnitude profile of the pellicle is relatively uniform and remains so up to 150 kHz. Above this, the pellicle profile becomes non-uniform and shows the on-set of modes which continue until around 400 kHz where the profile becomes relatively uniform again.

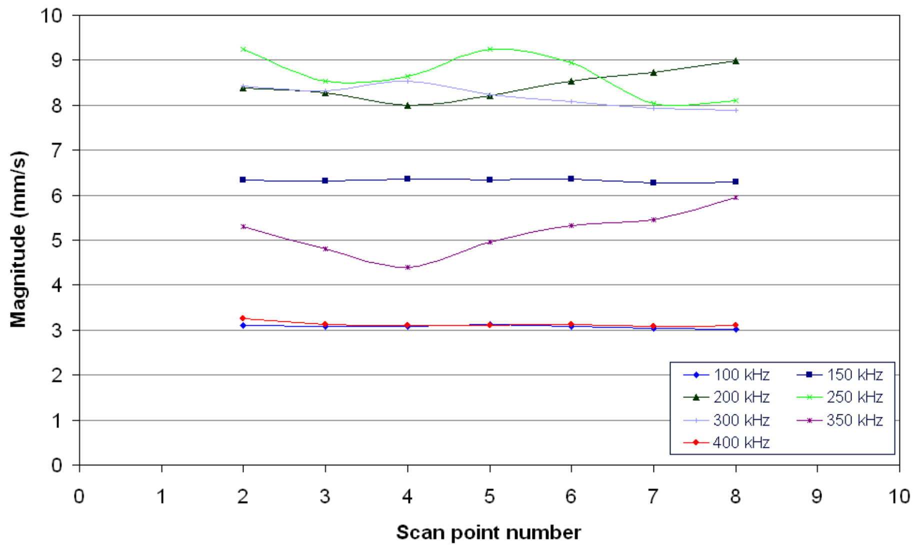

Figure 19. Velocity magnitude scans of 5 mm wide pellicle between 100 kHz and 400 kHz.

It can be seen from Figure 19 that the overall effect of the modes on the velocity measurement can be substantial, effecting the accuracy of the velocity measurement by as much as 30%.

It was also observed during the scans that the 0.23 m projector stand-off distance, not shown here, produced non-uniform behaviour that was worse than the 0.5 m stand-off distance results, particularly for the 10 mm pellicle. It was thought that the greater stand-off distance provided a more uniform (plane) wave-front and therefore a more uniform excitation of the pellicle.

2.5 High frequency measurements using strip pellicle

The work in section 2.4 highlighted the presence of flexural modes on the strip pellicle and section 2.3 showed the effect these modes had on the accuracy of a calibration using this technique. It was decided that reducing the width of the pellicle sufficiently might allow mode-free measurements to be performed up to 500 kHz, which is the upper frequency required from this project. Above this frequency, interferometry using the standard ring pellicle is well established. Measurements were performed in the small NPL test tank with the Polytec PSV 300 scanning vibrometer and two pellicles; one being 2 mm in width and the other being 1 mm in width.

2.5.1 Measurement procedure

The experimental arrangement used was similar to that described in section 2.3.1. The two pellicles were cut from the same sheet of aluminium (40 nm thick) coated Mylar (23 µm thick) and tensioned on the 1.3 m support frame described in section 2.2. A Panametrics 0.5 MHz piston transducer was used as the projector and excited with a 100 µs gated tone-burst between 300 kHz and 600 kHz. The PSV 300 scanning vibrometer was used to measure the point velocity of each pellicle on the acoustic axis of the projector such that the optical and acoustic beams were co-linear. The scanning function of the vibrometer was also used to measureme the velocity profile across the width of the pellicle at selected frequencies. The point velocity measurements were captured and digitised using a HP89410A vector signal analyser. The line profile scans were captured using the integrated data acquisition board of the PSV 300 and processed using the Polytec PSV software. The point measurements were also repeated using a Reson TC4034 as the reference hydrophone with a pre-amplifier gain of 5. Both the reference hydrophone output and the vibrometer output for the single point measurement were passed through a Krohn-Hite 3944 filter unit set with a filter width of 1 octave either side of the centre frequency.

2.5.2 Analysis of results

The single point velocity measurements obtained using the vibrometer were obtained using the nominal calibration factor for the sensitivity setting used (25 mm/s/V) and were compared with the derived velocity from the reference hydrophone measurement. As in section 2.3.3, the vibrometer was also used to provide an ‘optical’ calibration of the reference hydrophone which was then compared with the reference reciprocity data.

2.5.2.1 Results for 2 mm strip pellicle

The acoustic velocity measurements using the optical vibrometer and 2 mm wide pellicle are shown in Figure 20 along with the velocity measured using the TC 4034 reference hydrophone. The Reson TC 4034 is specified for absolute measurement up to 480 kHz by the manufacturer, although the reference device had been calibrated using reciprocity up to 600 kHz. Due to the active element diameter of the hydrophone (6 mm), it will suffer a small amount of phase cancellation at higher frequencies.

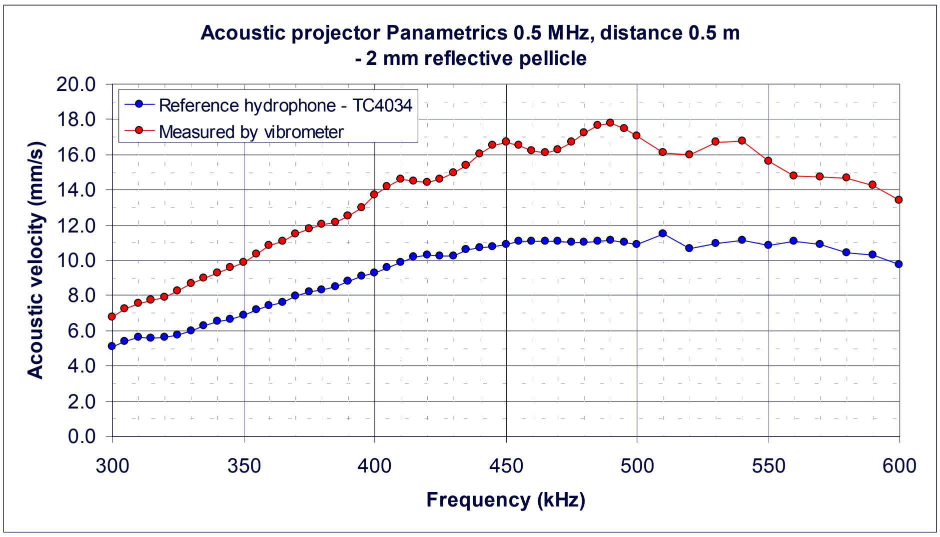

Figure 20. Acoustic velocity measurements using a TC4034 reference hydrophone and optical vibrometer using 2 mm wide pellicle.

The results using the 2 mm pellicle show evidence of modes above 380 kHz. This can be seen from the velocity deviations with frequency compared with the reference hydrophone data. The optical vibrometer velocity measurements also showed a considerable offset with those measured using the reference hydrophone. This was not believed to be associated with the pellicle as identical pellicle material was used in section 2.3 with a different vibrometer where overall agreement was good. Although the hydrophone might exhibit some phase cancellation at higher frequencies it was thought that the offset might have been associated with the nominal calibration factor of the vibrometer.

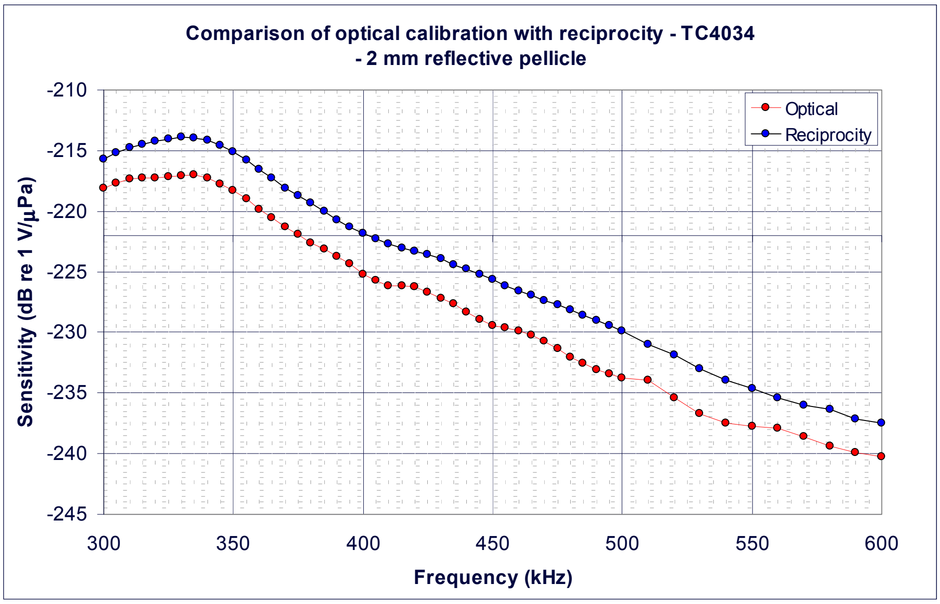

Figure 21. High frequency optical calibration results for the TC 4034 using 2 mm wide pellicle compared with its reciprocity reference data.

The use of a 2 mm pellicle reduced the effect of any modes on the hydrophone calibration up to 380 kHz and showed significantly less deviation from the reciprocity reference data (see Figure 21) than the results in section 2.3.3 with a wider pellicle at lower frequency.

2.5.2.2 Results for 1 mm strip pellicle

Repeat measurement results using a 1 mm wide pellicle are shown in Figure 22 and 23.

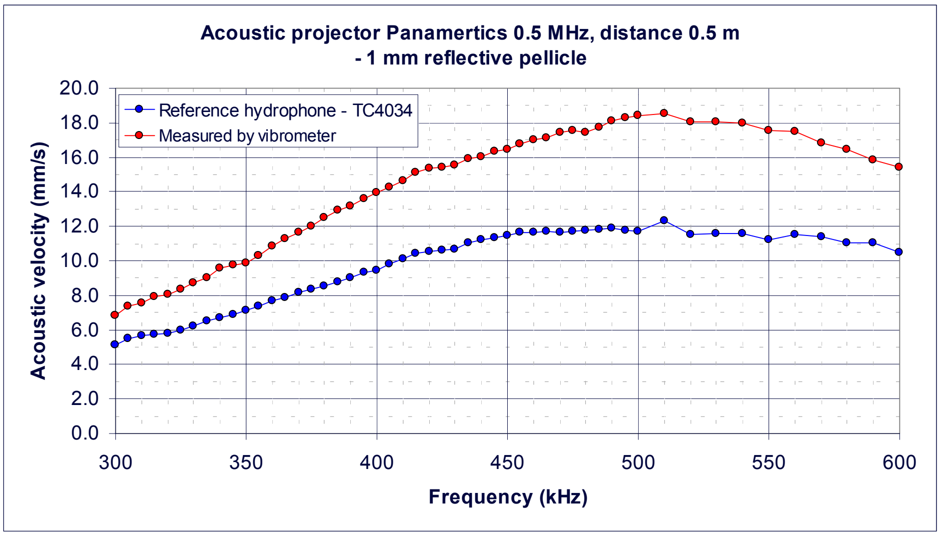

Figure 22. Acoustic velocity measurements using a TC4034 reference hydrophone and optical vibrometer using 1 mm wide pellicle.

The optical velocity measurement performed using the 1 mm pellicle showed no noticeable deviations in velocity with frequency (except for the overall offset discussed in section 2.5.2.1). This was particularly evident when comparing the sensitivities obtained optically and those obtained using reciprocity (see Figure 23). The small disagreements above 500 kHz could in fact have been due to the reference hydrophone, which was expected to suffer phase cancellation at these frequencies. Figure 24 shows a comparison between the Reson TC4034 reference hydrophone used in this work and Reson TC4035 reference hydrophone with a reduced active element diameter. This showed the acoustic velocity calculated from the output of each transducer. It can be seen that the TC4034 under-estimated the velocity at higher frequencies compared with the TC4035 which has a much smaller cylindrical active element, with a 1.5 mm diameter.

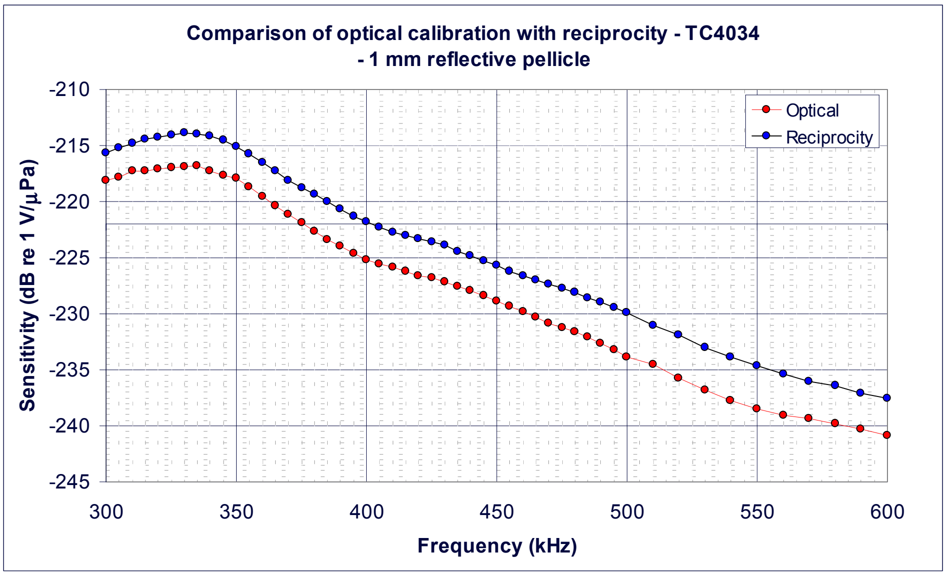

Figure 23. High frequency optical calibration results for TC 4034 using 1 mm wide pellicle compared with its reciprocity reference data.

The use of the Polytec scanning vibrometer in this section did not allow an accurate comparison between the optical method and the reciprocity method due to the inaccuracy of the vibrometer. However, section 2.3 demonstrated an agreement of around 0.5 dB between the optical and reciprocity method using a lower frequency vibrometer at frequencies where the calibration was not effected by pellicle modes. This current section further demonstrated that the use of a narrower pellicle (1 mm) allowed measurements up to 600 kHz with no noticeable effect from pellicle modes.

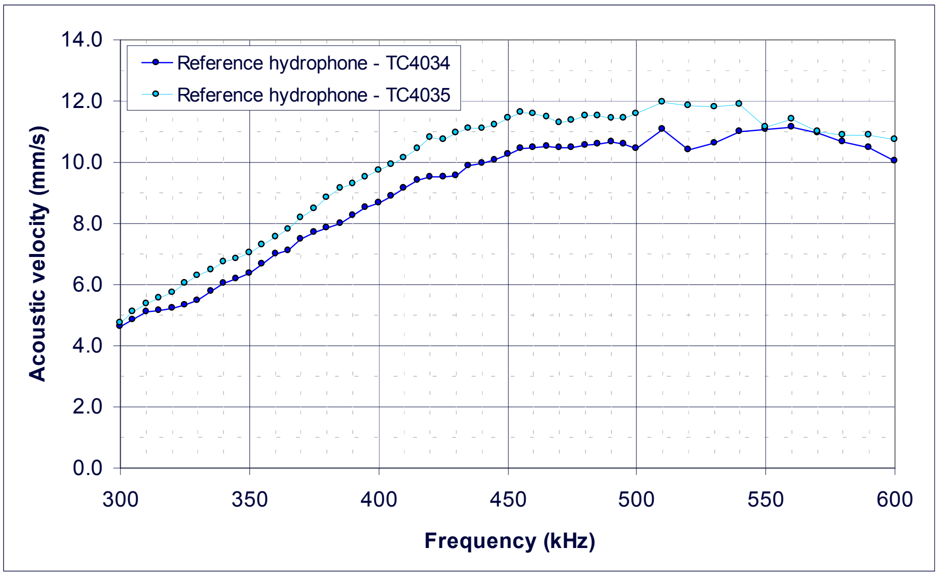

Figure 24. Comparison of acoustic velocity measurement using a TC4034 and a TC4035.

2.5.2.3 Scans of 1 mm and 2 mm pellicle

Surface scans were performed on the 1 mm and 2 mm pellicles over a range of frequencies and the line profiles of velocity magnitude between 400 kHz and 600 kHz are shown in Figure 25 for the 2 mm pellicle and Figure 26 for the 1 mm pellicle.

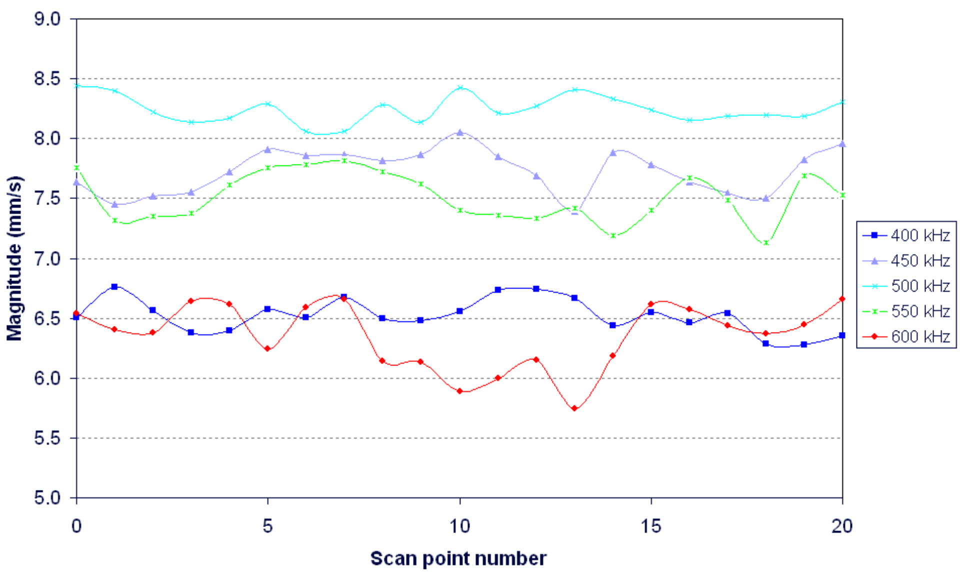

Figure 25. Velocity magnitude scans of 2 mm wide pellicle between 400 kHz and 600 kHz.

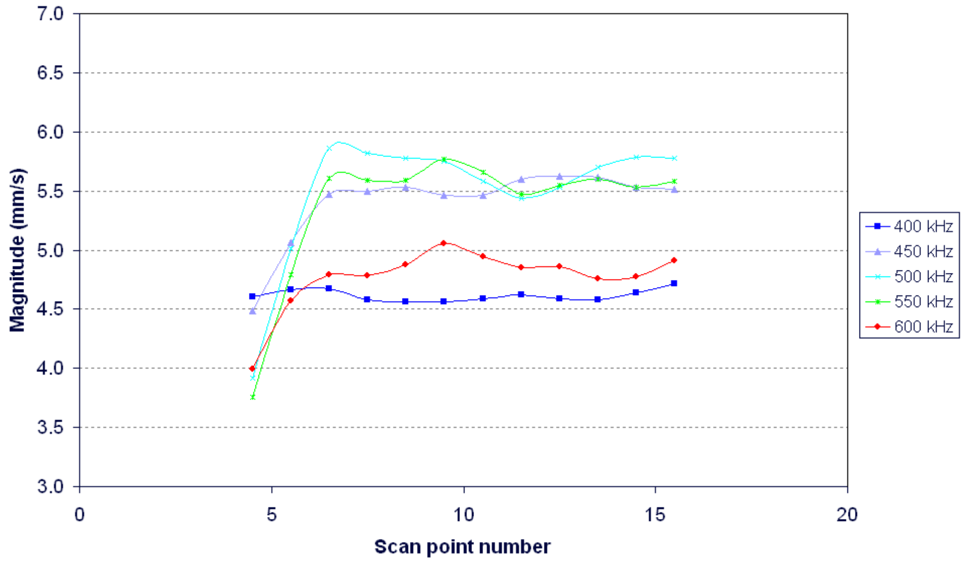

Figure 26. Velocity magnitude scans of 1 mm wide pellicle between 400 kHz and 600 kHz.

The 2 mm pellicle showed significant non-uniform behaviour at 400 kHz and above. At 400 kHz, the 1 mm pellicle was relatively uniform and even at higher frequency did not exhibit the non-uniform behaviour of the 2 mm pellicle. However, the 1 mm pellicle did show unexpected oscillations at the left hand edge of the strip (see Figure 26). It is thought that this was caused by a serrated edge on the pellicle where it had been cut, leading to a tension free pellicle edge. It should also be noted that these are magnitude plots and so do not truly represent the oscillatory behaviour of the pellicle motion.

Overall, the results in this chapter have demonstrated that a 1 mm strip pellicle provides the capability to calibrate a hydrophone up to 600 kHz without any noticeable deviations caused by pellicle modes. The surface scans of the 1 mm pellicle further demonstrate that the variations across its width are generally small except at the pellicle edge. The use of specially prepared aluminium coated tape with straight edges could significantly reduce the edge effects and possibly reduce the overall non-uniform behaviour of the pellicle. This was observed in section 2.3.3.1, where the 12.6 mm wide video tape provided much greater stability than the 10 mm cut aluminium coated Mylar of similar thickness in section 2.3.3.3.

The effect of the pellicle modes in acoustic fields of lower pressure could not be tested due to the limited noise performance of the Polytec scanning vibrometer. However, the measurements in section 2.3 show good agreement with a reference hydrophone at lower frequencies for measurement of smaller velocities. A small amount of further work is planned which will test the 1 mm pellicle over an extended frequency range from 5 kHz to 500 kHz and thus asses its capability at lower frequencies. The use of one pellicle for an extended frequency range would be advantageous. Work is also planned to assess the suitability of the 1.3 m pellicle support frame at lower frequencies.

3 ALL FIBRE HETERODYNE INTERFEROMETER

3.1 Advantages of developed heterodyne interferometer

The justification for a heterodyne interferometer and the reasons for opting to use a fibre-based system were explored in detail in the Phase Two report [2]. Following developments and optimisations to the all-fibre heterodyne interferometer and experience gained using commercial vibrometer systems during Phase Three of the project, a detailed list of advantages of the developed interferometer has been compiled.

i. Commercial systems are effective black box units which if and when calibrated are done so against vibration standards similar to accelerometers. Hardware and software signal processing is used with many interdependent options making the interpretation of measured signals complex which limit traceability. The all-fibre interferometer developed for this project is modularised to allow characterisation of every stage. Measurement of the Doppler signal provides traceability to the wavelength of light, meaning that traceable measurement of the Doppler frequency shift allows traceable measurement of acoustic velocity. The Doppler decoder stage on the all-fibre vibrometer can be calibrated against existing frequency standards.

ii. The heterodyne configuration coupled with optical Doppler measurement provides far greater low frequency stability than a standard phase or homodyne interferometer.

iii. The use of Doppler analysis overcomes the linear dynamic range limitations of phase locked phase interferometers.

iv. Measurement of the Doppler shift further makes the interferometer more robust to environmental conditions that may affect the light level.

v. All commercial vibrometers are based on 633 nm laser light which is not suited for propagation in water. The developed all-fibre heterodyne interferometer uses a 532 nm laser source for low attenuation in water. Using 532 nm also allows an Nd:YAG laser to be used in place of a standard He-Ne laser. This allows single frequency mode operation at much higher power levels than is possible with a He-Ne type. The all-fibre design would not be feasible with the power available from a frequency stabilised He-Ne laser.

vi. The Nd:YAG laser has a much greater coherence length than a He-Ne laser and so the all-fibre interferometer does not exhibit sensitivity variations (noise floor level) with stand-off distance; an effect which is experienced on commercial vibrometers.

vii. The all-fibre design provides greater robustness to environmental conditions and gives the potential for operation underwater.

viii. The all-fibre interferometer makes us of fibre that does not maintain the polarisation of the light. Although this makes isolation of back reflection to the laser more technically challenging, it also means that the interferometer is not hindered when collecting de-polarised light from a target. Scattered light from a diffuse surface can be described using Lambert's cosine law of diffusion [3]. For this type of scattering surface the returned light level is reduced because of this diffusion but in addition to this, the light is also completely depolarised. Commercial vibrometer and interferometer systems use polarising beam splitters to separate the returning light component to combine with the reference arm. If the reflected light from the acoustic target is depolarised, the AC component separated for producing the Doppler signal will be significantly reduced (even if a large amount of light is collected) and lead to an increased noise floor at the Doppler decoder output. In such an application, the all-fibre interferometer would only be affected by the light level loss due to Lambertian scattering and would use all the available returned light to produce the Doppler signal.

ix. Commercial vibrometers are marketed for the purpose of vibration measurement as a robust alternative to accelerometers and are therefore designed for high velocity applications. These velocities may extend from a few mm/s to several m/s. For underwater measurement, a much smaller dynamic range is required from fractions of a mm/s to a maximum of 10 mm/s.

x. Generally, commercial devices do not offer the required frequency range with the sensitivity required in this project. The all-fibre heterodyne interferometer is designed to operate specifically within in the acoustic bandwidth require (1 kHz to 500 kHz).

3.2 Improvements to heterodyne interferometer

3.2.1 Prototype system

Several changes have been made to both the optics and electronics of the interferometer during Phase Three of the project. Progress on the interferometer was heavily detailed in the Phase Two report [2] so this section only considers changes implemented during Phase Three of the project.

3.2.1.1 Split ratio of interferometer arms

The initial prototype system reported in the Phase Two report [2] used a 50/50 coupler which divided the laser light into the signal arm and the reference arm equally. The maximum interference signal is obtained when the light is split equally between the signal and reference beams. However, the losses in the signal arm were significantly greater than those in the reference arm due to the transmission and collection to and from the target. This resulted in a dominant reference DC level on the photodiodes with only a small AC component. To overcome the losses in the signal beam the 50/50 coupler was replaced with a 90/10 coupler which sends 90% of the light intensity into the signal arm and the remaining 10% into the reference arm. This increased the depth of modulation on the interference signal by providing an increased AC to DC level, whilst maintaining a dominant reference DC level. In practice, it is common to have a larger reference arm intensity level to provide an increased signal level to photon noise ratio at the photodiode.

3.2.1.2 Increased light level

The overall light level in the system has been increased by moving to a 100 mW short cavity Nd:YAG laser. This doubles the light level over the existing laser and also increases coupling efficiency into the fibre. There are still improvements to be made with the ‘pigtailed’ launch fibre from the laser and stability should be improved by the use of a polarising isolator.

3.2.1.3 Transmit-collection optics

The delivery optics of the prototype interferometer have been modified to deliver and collect along the same optical path. The previous version of the interferometer used a separate delivery fibre with a collimator lens and collection fibre with a focussing lens. This previous system had a number of disadvantages:

- The two beam arrangement made alignment of the optics very difficult.
- The incident beam falls on the acoustic target at an angle to the normal and would therefore require a cosine correction based on an estimate of the incident angle.
- Both the incident beam and the returning beam propagated through the water with a non-zero angle of incidence to the acoustic wavefront. This means that regions of varying refractive index (the acoustic beam) are crossing the optical beam. This acousto-optic effect has been discussed in the Phase One report [1] and has been used to measure acoustic fields non-invasively [12] [13]. This effect would introduce errors into the pellicle velocity measurement.
- The differing propagation paths through the acoustic field would make any correction for the acousto-optic effect erroneous.

The single beam modification employs a ‘bulk optic’ telescope system to expand the beam from the fibre and then focus the beam as a point on the target. The telescope is a reversible system so any light that is collected by the collection lens from the target is re-focussed into the fibre. A diagram of the system is shown in Figure 27.

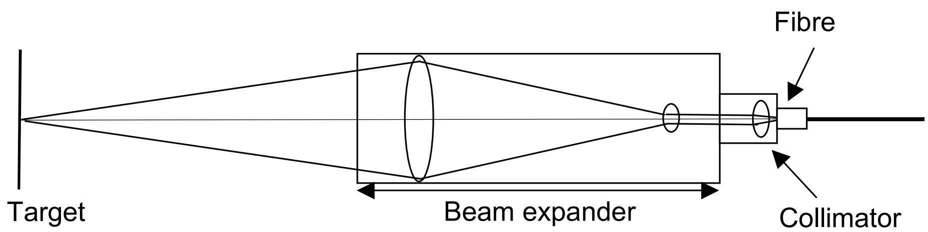

Figure 27. Front-end single beam optics.

To enable this optical front-end system to work, it is essential to redirect the returning light down a different path to that of the incident light. This is achieved by the use of a 50/50 coupler just before the telescope system and allows the returning light to be re-combined with the reference arm in the mixing coupler. The disadvantage of the 50/50 coupler is that it is completely reversible and therefore discards 50% of the light on the incident path and splits the returning light evenly between the path to the mixing coupler and the path back to the laser source; a total loss of 75%. The current system employs this configuration successfully, although isolation to the laser needs to be improved for greater frequency and intensity stability. A diagram of the current system is depicted in Figure 28 showing the coupler in the signal arm.

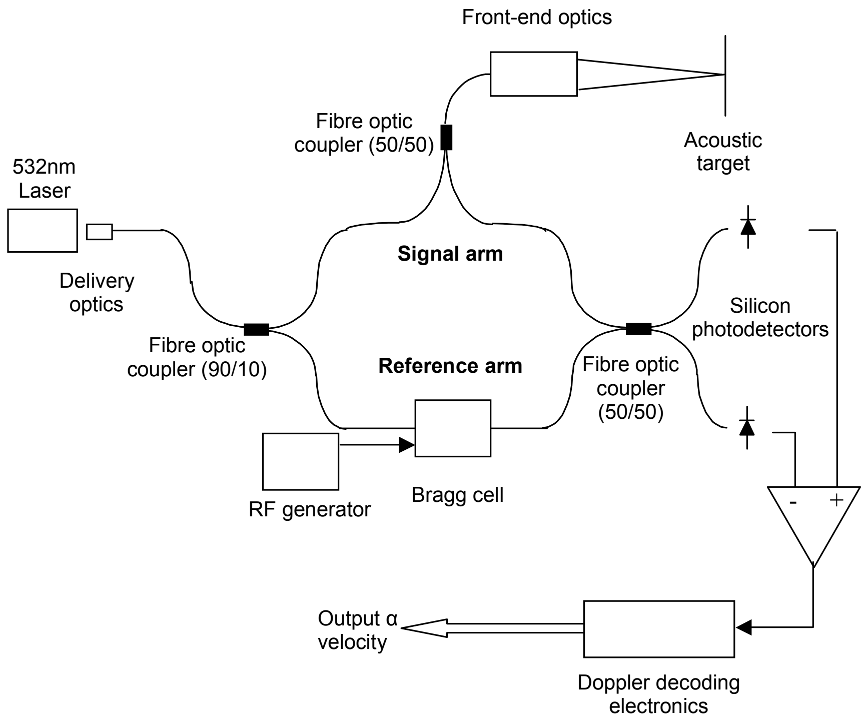

Figure 28. Diagram of current all-fibre heterodyne system.

3.2.1.4 Doppler decoding

The Doppler decoding electronics shown in Figure 28 has been completely modified since the end of Phase Two and now includes a Phase Locked Loop circuit (PLL) to track the Doppler shift frequency. The PLL circuit provides an output voltage proportional to the Doppler frequency shift and thus the target velocity. A block diagram of the hardware signal processing between the photodiode stage and the demodulated output stage is shown in Figure 29.

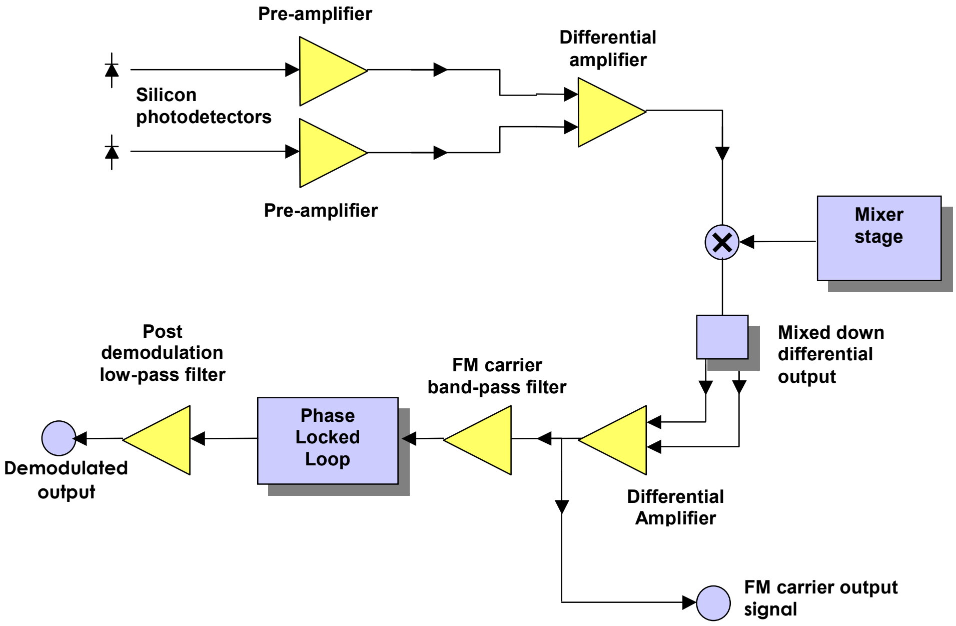

Figure 29. Block diagram of hardware signal processing applied to the FM heterodyne signal.

The hardware signal processing has been optimised to avoid any impedance mismatches and employs differential amplification where possible to reduce coherent noise. The mixer stage reduces the FM carrier signal from the photodiodes to a more manageable frequency before demodulation. The PLL stage then tracks the Doppler frequency shift to produce a linear output with a bandwidth greater than 500 kHz.

3.2.2 Final system

The final system will build on many of the modification made to the prototype in Phase Three with the aim of increasing overall light level and reducing the electronic noise floor. The current system already provides the basis for the required dynamic range and frequency range, although recently developed electronics will be added to increase overall performance. The final system will also include an additional optical head that will be hermetically sealed for operation in water up to 5 metres deep. The final system will also be constructed in modular form allowing changes to the electronics for increased scope in future applications. For example, the phase look loop circuit itself could allow an acoustic bandwidth greater than 2 MHz with the correct filters and will also allow a dynamic range far beyond the 5 mm/s required. If required, the dynamic range could be increased by extending the pass-band of the FM carrier band-pass filter to allow velocities of up to 600 mm/s to be measured.

The system will also include a calibration port where a frequency standard can be used to calibrate the instrument electronically.

3.3 Comparison with a reference hydrophone

Measurements were performed in the NPL small test tank using a 2 mm strip pellicle and the all-fibre heterodyne interferometer. The measurements were performed to assess the overall performance of the phase three interferometer. A reference hydrophone was used to provide an independent validation of the velocities measured using the interferometer. The velocities measured were also used to calibrate the hydrophone which were then compared with the reciprocity reference calibration data for the same hydrophone.

3.3.1 Measurement procedure

The measurement procedure was very similar to that used in section 2.3.1 where the interferometer was positioned using a camera tripod such that the laser beam entered the test tank through the access window shown in Figure 2a. The optical beam was first positioned on the acoustic axis of the acoustic projector such that the optical and acoustic beams were co-linear; the pellicle was then inserted in the path of the optical beam such that the projector to pellicle separation was 0.5 m. The optical beam was then reflected from the pellicle, returning to the collection lens on the interferometer head, with the electrical signal output of the interferometer digitised using a HP89410A vector signal analyser.

The pellicle used was a 2 mm strip of Mylar of thickness 23 µm coated on one side with 40 nm of aluminium stretched over the 1.3 m aluminium frame shown in Figure 1. The pellicle frame was positioned approximately 325 mm from the access window as shown in Figure 30. This shorter stand-off distance from the window served to reduce losses due to scattering in the water, which was increased due to local temperature variations. The hydrophone measurements were also performed for the same projector/receiver position.

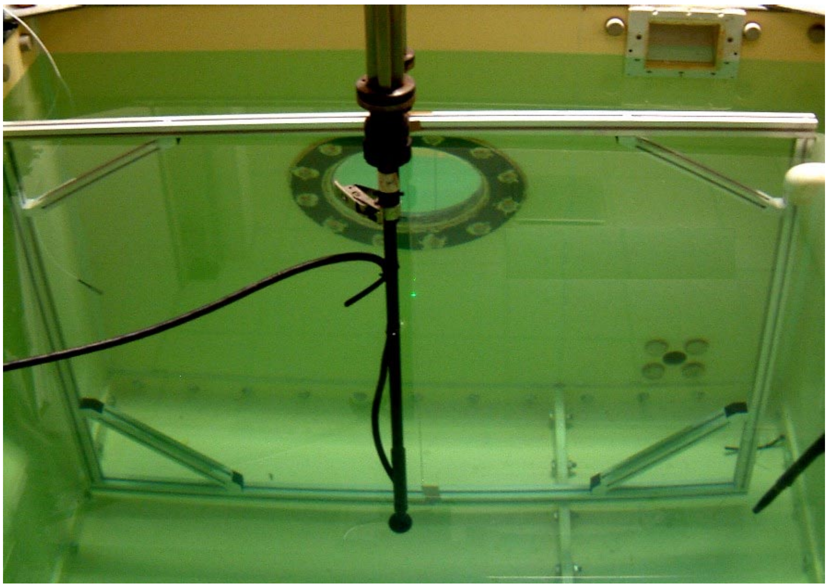

Figure 30. Optical setup using ITC1042 projector.

Three transducers were used as acoustic sources for a series of measurements:

- ITC1042 – a 25 mm diameter sphere with a resonance at 75 kHz, used in the range 40 kHz to 120 kHz.
- Panametrics piston – 1.5” diameter piston transducer with a resonance of 0.25 MHz, used for the range 100 kHz to 400 kHz.
- Panametrics piston – 1.0” diameter piston transducer with a resonance of 0.5 MHz, used for the range 300 kHz to 600 kHz.

The acoustic projectors were driven with time-gated tone-bursts of around 0.26 ms in length and signal amplitudes of around 80 $V_{p\text{-}p}$, using a HP-331020A function generator coupled to a power amplifier. A B&K 2713 50 dB power amplifier was used for the ITC1042 projector and an ENI 240L 50 dB power amplifier was used for both Panametrics projectors. The captured signal was time windowed to isolate the acoustic reflections such that measurements were only made on the steady-state portion of the direct path signal. In each case, an NPL TC4034 reference hydrophone was used to provide an independent measure of the acoustic output of the source. This had previously been calibrated by the reciprocity method.

The interferometer was aligned to provide maximum reflection from the pellicle. This was achieved by monitoring the voltage of the FM carrier signal generated by the interferometer before demodulation. In general, a greater carrier amplitude provides improved signal-to-noise in the demodulated signal. Measurements were then made of the steady-state acoustic signal using the demodulated output of the interferometer phase locked loop (PLL) stage at a range of frequencies. To provide velocity information, it was necessary to calibrate the PLL stage of the interferometer to obtain absolute Doppler shift information and thus velocity from the output voltage (this procedure is described in section 3.3.2). The hydrophone was then positioned in the acoustic field such that the optical beam was incident on the acoustic centre of the hydrophone. The steady-state acoustic velocity was then calculated from the measurements of acoustic pressure made with the reference hydrophones (the calculations were performed using the plane-wave relationship between acoustic pressure and acoustic particle velocity) for the same frequencies. A Krohn-Hite 3944 band-pass filter unit was used on the output of both the interferometer and the hydrophone, using a band-pass of one third of an octave and an octave, either side of the drive frequency respectively. The hydrophone output was further coupled to a unity gain buffer amplifier. The outputs from the interferometer and the hydrophone were captured and digitised using a HP89410A vector signal analyser. To further improve signal-to-noise ratio of the interferometer signals, 2 measurements were performed each obtained using 40 on-board time averages, where the average of the 2 measurements was used. This repeat procedure was used to ensure agreement between successive measurement sets.

A comparison was then possible between the acoustic velocity measured using the heterodyne interferometer and those obtained from the reference hydrophone. The sensitivity of the reference hydrophone was also calculated using the optical measurement data and compared to the reference reciprocity data for the same hydrophone. This procedure was repeated using the different acoustic projectors to cover an extended frequency range. The comparison results are presented in section 3.3.5.

Measurements were also performed using the vector signal analyser of the noise spectra obtained from the output of the vibrometer without the acoustic signal present (these results are shown in section 3.3.4)

3.3.2 FM calibration of PLL stage

The phase locked loop stage of the interferometer provides an output voltage proportional to the Doppler shift on the carrier frequency that results from the acoustic modulation of the heterodyne frequency. It was described in the Phase Two report [2] how measurement of the Doppler shift allows the acoustic velocity to be determined absolutely. To establish the voltage produced at the PLL output for a given Doppler shift, the velocity demodulation processing end of the interferometer was calibrated using an injected FM signal of known modulation depth provided by a Marconi Instruments 10 kHz – 1 GHz signal generator 2022E.

The calibration procedure was to inject an 80 MHz FM signal into the post photodiode pre-amplifier stage with a 9.6 kHz maximum excursion from the carrier and with a variable modulation frequency, which would represent the peak Doppler shift and the acoustic frequency respectively. The RMS output voltage from the PLL stage was then measured using a Tektronix spectrum analyser for a series of modulation (acoustic) frequencies between 1 Hz and 600 kHz. The response of the interferometer electronics to the 9.6 kHz peak Doppler shift was then found as a function of frequency and plotted as a calibration factor with units of velocity per unit voltage as shown in Figure 31.

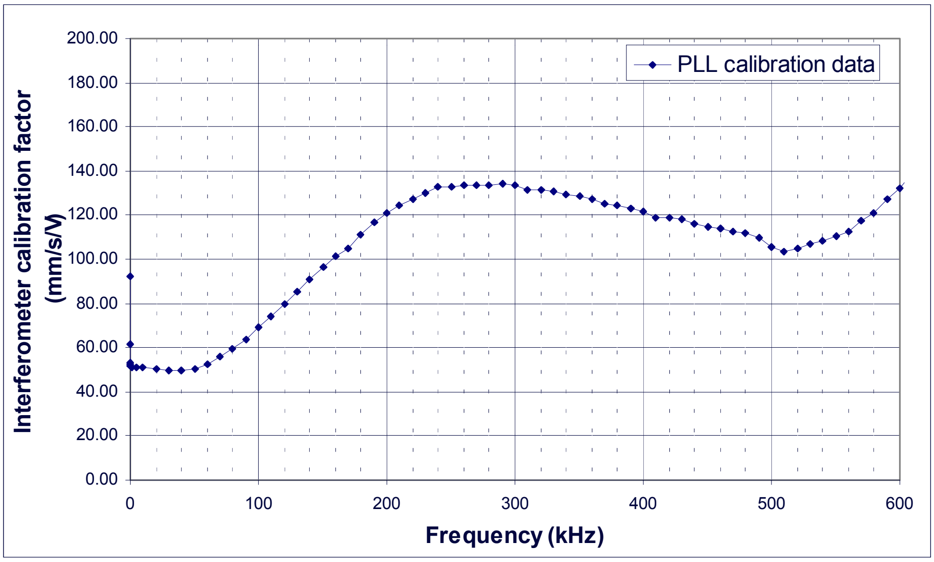

Figure 31. Interferometer calibration chart.

Figure 31 shows that the interferometer is most sensitive between 10 Hz to 100 kHz and is least sensitive around 280 kHz. The Doppler decoding arrangement used for these measurements employed a 78.5 MHz mix down frequency at the mixer stage to provide a 1.5 MHz carrier for demodulation. Further revisions of the PLL stage aim to increase the carrier frequency to provide better broadband performance.

3.3.3 Optical power readings

Measurements were performed to assess the optical performance of the interferometer when aligned on the 2 mm pellicle in the NPL small tank. Although the output from the telescope front-end discussed in section 3.2.1.3 remains constant irrespective of the measurement environment, the amount of light returned in to the interferometer depends on the condition of the access window, the propagation distance through the water and the reflectivity of the pellicle. This directly effect the DC to AC ratio and thus the noise performance of the interferometer. A Coherent labmaster laser power meter was used to measure the light power transmitted from the front-end telescope optics and the light level incident on the photodiodes. The light level on the photodiodes was measured firstly with the Bragg cell (reference arm) switched off which allowed the AC component power to be measured, and secondly with the light beam from the telescope (signal arm) blocked to allow only the DC component to be measured.

The laser light transmitted to the target was measured at 1.3 ± 0.1 mW, the DC component incident on a single photodiode was 3.9 ± 0.3 μW and the AC component incident on a single photodiode was 4.8 ± 0.3 μW. It should be noted that the interferometer uses a diode pair arrangement with the incident light split evenly between the two photodiodes. The overall light level incident on the photodiodes is therefore twice that measured on a single photodiode. Therefore, around 1 % of the light in the signal beam that exits the telescope is collected back and directed to the photodiode and 99.98% of the initial 100 mW laser power is lost through the system. Many of these losses could be reduced and should lead to significant increases in the overall light level on the photodiodes and thus reduce the velocity equivalent noise floor of the interferometer.

3.3.4 Velocity equivalent noise floor

The noise floor was captured with the interferometer aligned on the pellicle in water as described in section 3.3.1 and no acoustic signal present. The Krohn-Hite band-pass filter was used to limit the measurement bandwidth between 200 kHz and 300 kHz where the response of the interferometer was relatively flat. An average calibration factor in this frequency range was used to provide a noise floor plot showing the equivalent velocity as shown in Figure 32.

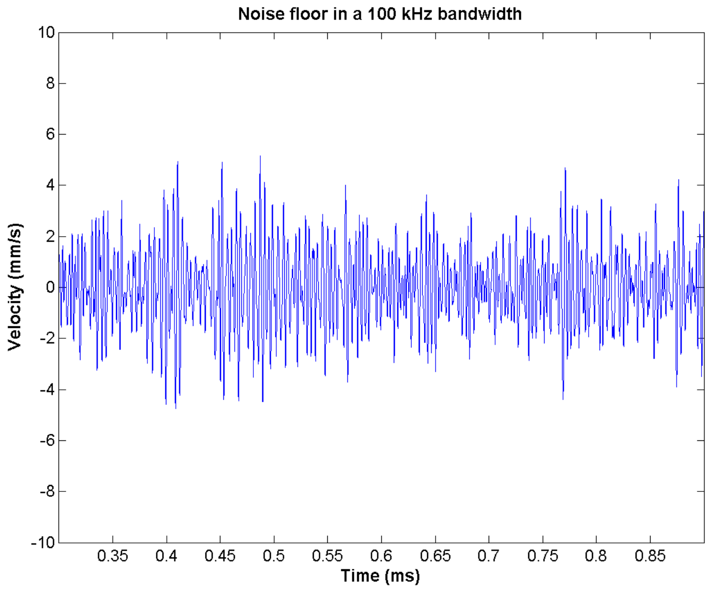

Figure 32. Captured time signal with no acoustic source present.

The noise equivalent velocity spectrum has also been plotted in Figure 33 for comparison against the noise equivalent spectrums obtained using the Polytec CLV-1000 vibrometer shown in Figure 3.

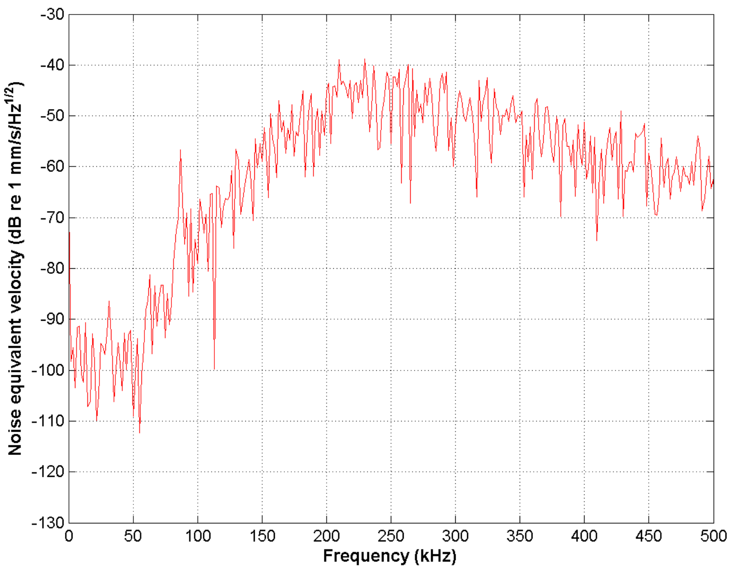

Figure 33. Noise equivalent velocity spectrum of interferometer with a 200 kHz to 300 kHz band-pass filter.

Comparing Figure 33 with Figure 3 shows that the all-fibre interferometer has a noise equivalent velocity of around an order of magnitude greater than that of a Polytec vibrometer under similar conditions, although the Polytec results were obtained with a less reflective tape pellicle. An improvement of around 400 times is required to meet the noise equivalent RMS velocity of 10 µm/s in a 200 kHz bandwidth with no averaging, as specified for the project.

3.3.5 Comparison results

The results using the ITC1042 projector for acoustic frequencies between 40 kHz and 120 kHz are shown in Figures 34 and 35. Figure 34 shows the comparison between the velocity measured by the interferometer using the PLL calibration data shown in Figure 31 and the velocity calculated from the output of the reference TC4034 hydrophone. Figure 35 shows the sensitivity of the TC4034 hydrophone calculated using the interferometer velocity information compared with the actual reference reciprocity sensitivity data.

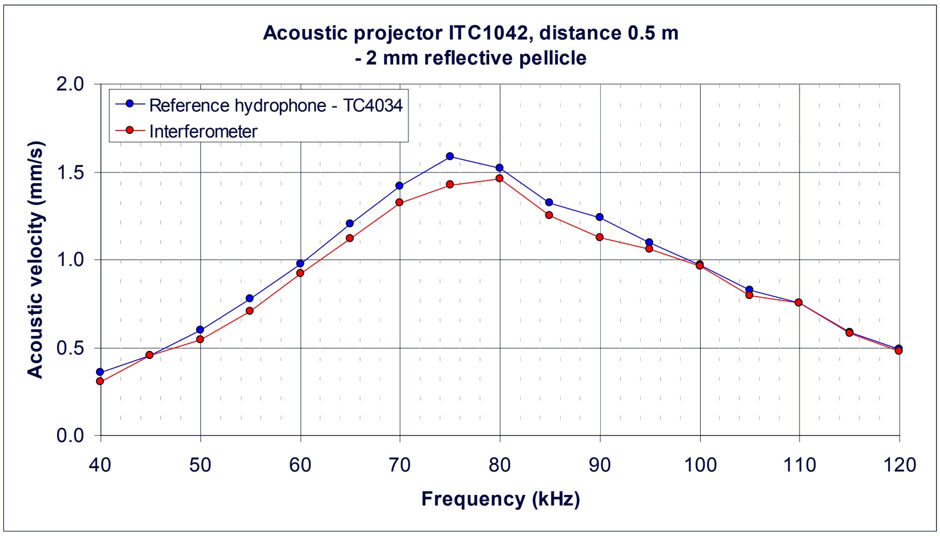

Figure 34. Comparison of velocity measurements using the TC4034 hydrophone and the heterodyne interferometer between 40 kHz and 120 kHz.

Figure 35 shows a disagreement of around 1 dB or more from 40 kHz to around 55 kHz where the disagreement reduced to around 0.5 dB until 100 kHz where the agreement improved to less than 0.5 dB at 120 kHz. The reason for poorer agreement at lower frequency was unknown.

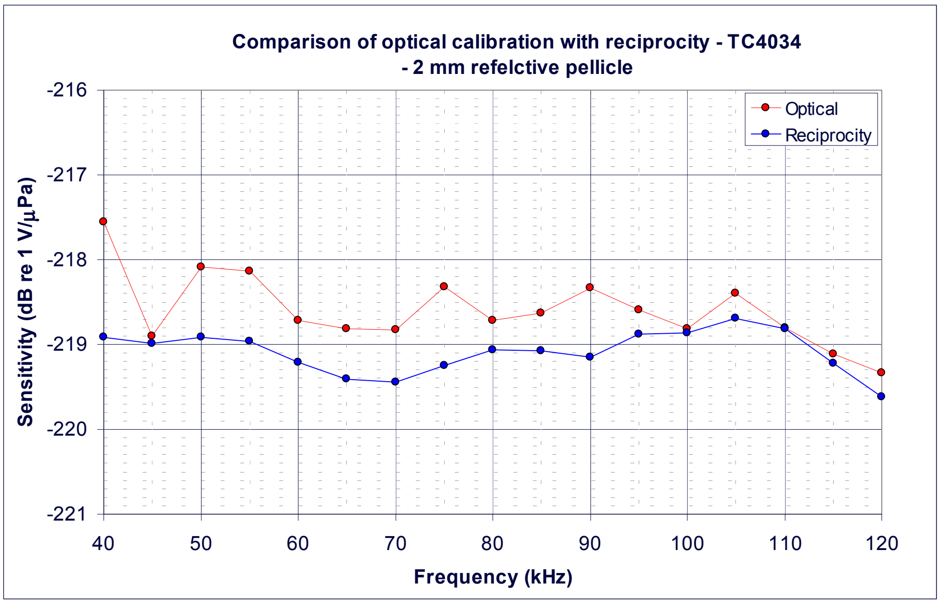

Figure 35. Calibration results of TC4034 hydrophone between 40 kHz and 120 kHz using the optical method compared with the reference reciprocity data.

The measurement results between 100 kHz and 400 kHz using the 0.25 MHz Panametrics projector are shown in Figures 36 and 37. From 100 kHz the agreement is similar to that seen using the ITC1042 projector, around 0.5 dB up to around 250 kHz. Beyond 250 kHz the interferometer and the hydrophone measurements progressively start to disagree, with a disagreement of over 2 dB at 400 kHz. It was suspected that this disagreement might have been due to the frequency limitation of the PLL, or more specifically the use of a 1.5 MHz carrier frequency. As shown in the Phase Two report, the FM signal contains a series of sidebands spaced at multiples of the acoustic frequency away from the central carrier. The number of sidebands and the amplitude of each would primarily depend on the modulation depth or in this case, the acoustic drive level. It was thought that at higher frequencies, above 250 kHz for example, some of the sidebands could be approaching the 1.5 MHz limit and folding back; causing loss of information at the demodulation stage. At 250 kHz, this would begin to happen if more than 6 sidebands were present. The effect may have been reduced by using a lower drive level on the projector, thus decreasing the amplitude and number of sidebands.

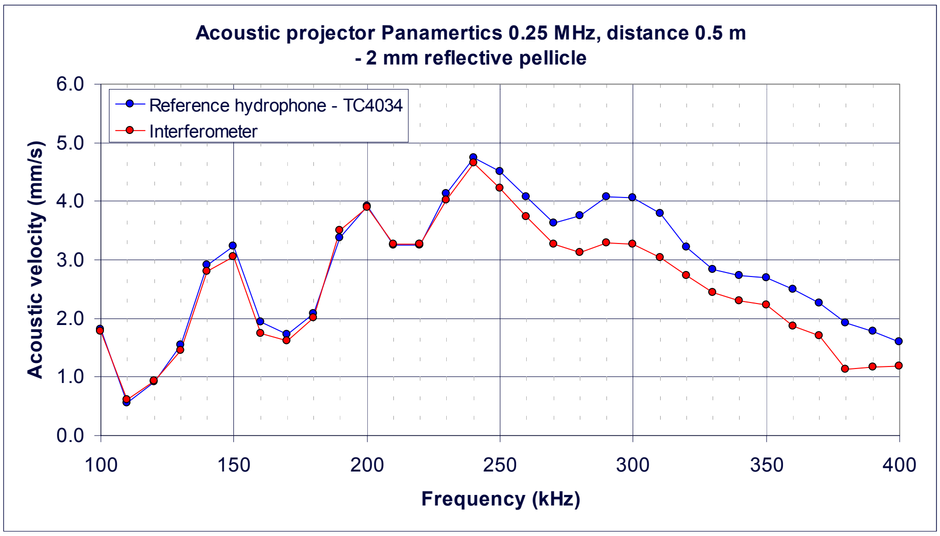

Figure 36. Comparison of velocity measurements using the TC4034 hydrophone and the heterodyne interferometer between 100 kHz and 400 kHz.

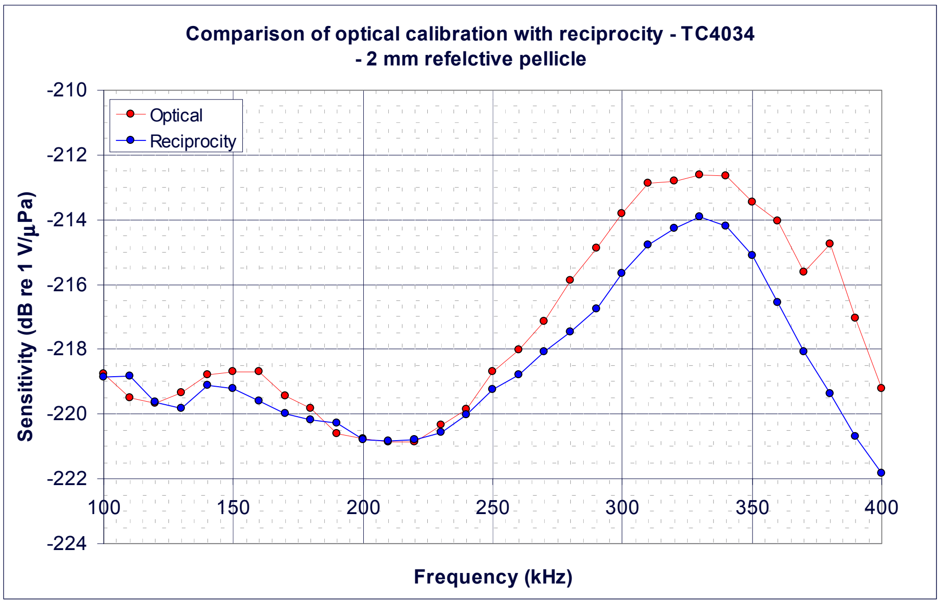

Figure 37. Calibration results of TC4034 hydrophone between 100 kHz and 400 kHz using the optical method compared with the reference reciprocity data.

Higher frequency measurements between 300 kHz and 600 kHz using the 0.5 MHz Panametrics projector continue this trend of increasing disagreement between the interferometer and hydrophone with increasing frequency (see Figures 38 and 39). At the upper specified frequency of 500 kHz the disagreement is around 6 dB.

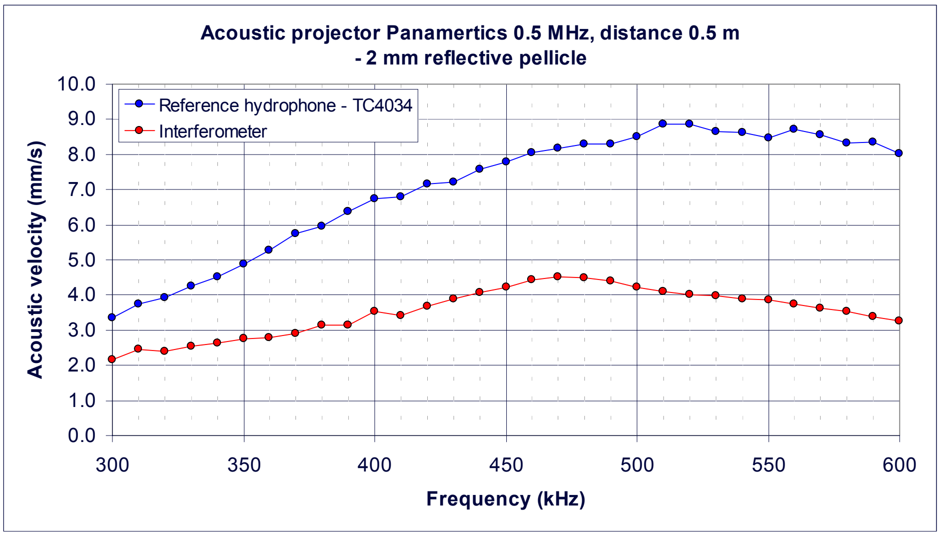

Figure 38. Comparison of velocity measurements using the TC4034 hydrophone and the heterodyne interferometer between 300 kHz and 600 kHz.

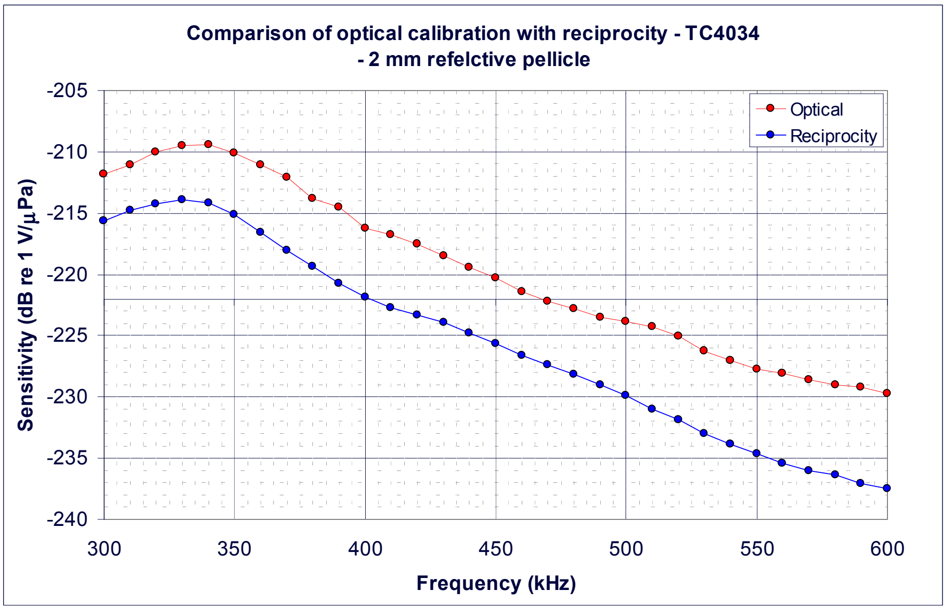

Figure 39. Calibration results of TC4034 hydrophone between 300 kHz and 600 kHz using the optical method compared with the reference reciprocity data.

3.3.6 Discussion

The Phase Three comparison results between the new all-fibre heterodyne interferometer prototype and a TC4034 reference hydrophone were encouraging below 300 kHz, with some small disagreement, particularly below 60 kHz. However, the new optical device appeared limited at frequencies above 300 kHz and showed significant disagreement with the reference hydrophone which was independently verified at higher frequencies against a reference TC4035 hydrophone (see Figure 24). It was thought that the high frequency limitation of the device was related to the PLL stage and the 1.5 MHz carrier that it utilises. It is planned to address this limitation by an improved PLL stage using a higher carrier frequency. Improvements are also planned to increase the overall light level and decrease the noise equivalent velocity. It is planned to increase the overall light level and thus reduce the noise floor by optimising the laser coupling into the delivery fibre. Further improvements to increase collection efficiency of the laser light from the target are planned by modification to the front-end delivery/collection optics. These improvements, coupled with continuing optimisations to the electronics should yield significant improvements to the noise equivalent velocity and allow accurate velocity measurement beyond 500 kHz.

4 NEAR FIELD CHARACTERISATION OF UNDERWATER TRANSDUCERS

4.1 Near field measurements

For transducers and arrays that are many acoustic wavelengths in dimension, it is not always possible to make the desired measurements in the acoustic far field within a laboratory tank of finite size. An alternative is to make measurements in the acoustic near field of the transducer and then calculate the far field response using appropriate propagation methods [14]. The measurements require that the magnitude and phase of a field parameter such as acoustic pressure (or particle velocity) be measured over a surface that captures the entire acoustic field. The field may also be back propagated to the transducer face to determine the source distribution, a technique which can be a useful diagnostic tool when characterising the performance of transducers or arrays since any defects may then be identified. The nature of the propagation methods are beyond the scope of this report and so are not described here.

The near field measurements are typically undertaken by use of a small hydrophone to measure complex acoustic pressure, the hydrophone being scanned through the field and measurements made at discrete points. For high frequency directional beams, a planar surface scan is typically undertaken, with care taken to sample over a wide enough area to capture the whole beam, and with a small enough spatial increment that the field is sufficiently sampled (typically 1/3 of a wavelength or better is required).

Optical techniques provide an alternate method of undertaking near field scans, which may offer potential advantages over traditional hydrophone scanning.

4.2 Acoustic near field scans

The scans described here were performed on a circular transducer with a diameter of approximately 150 mm. The transducer usually makes up part of a parametric array and was driven with a tone burst frequency signal of 320 kHz.

4.2.1 Optical scans

The Polytec scanning vibrometer described in section 2.4 was used to perform the acoustic near field scans of the transducer. Two different types of scan were performed, one scan was made using a wide pellicle suspended 10 mm from, and parallel to, the face of the transducer and the vibrometer scanned an area of the pellicle corresponding to the face of the transducer. The second type of scan was undertaken by reflecting the laser beam of the vibrometer directly off the face of the transducer, which was reflective enough to scan effectively. All scans were performed in the NPL small tank.

The near field of an acoustic source may be considered to exist for a distance D^2/λ in front of the transducer, where D is the largest lateral dimension of the active element of the transducer and λ is the wavelength. Using this equation, the near field of the transducer was calculated to be approximately 4.8 m, the scans using the pellicle were performed with the pellicle suspended 10 mm away from the face of the transducer, well within the transducer's near field. The transducer was driven at a frequency of 320 kHz using a HP33120A function generator at 600 mVp-p and an ENI 240L power amp at 50 dB. The measurements were taken using acoustic tone bursts of 25 cycles with the function generator triggered by the

Polytec scanning vibrometer at a frequency of 10 Hz. The pellicle was positioned centrally in the tank, aligned with the tank optical window. The scan area was set at 180 mm by 180 mm and contained 34780 scan points, which gave a resolution of approximately 1 mm.

In Figure 40, the acoustic near field scan is shown in terms of particle velocity magnitude at a frequency of 320 kHz. The circular face of the transducer is obvious in the scan, also clearly visible are four ring-like artefacts.

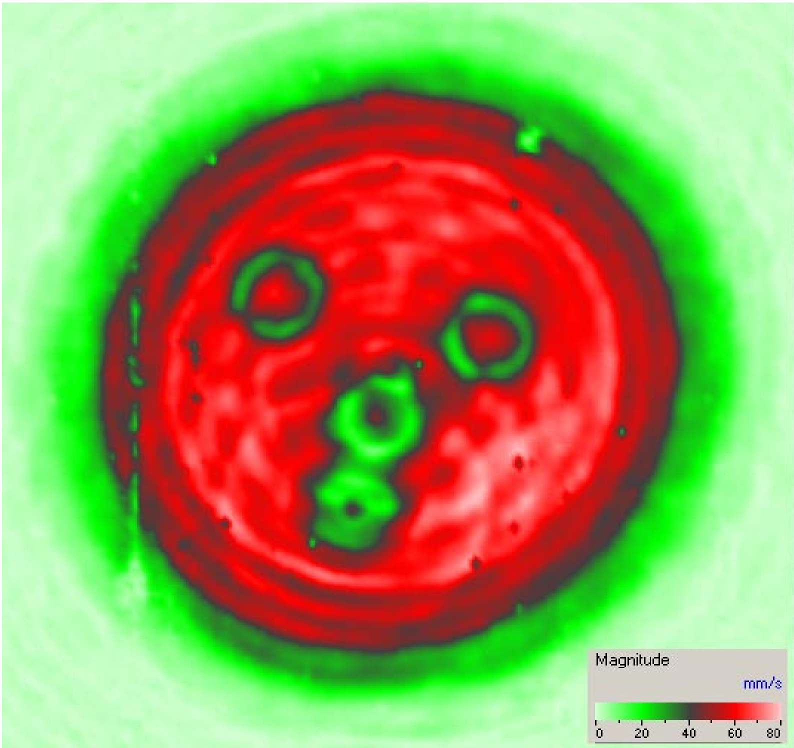

Figure 40. Magnitude (in mm/s) of acoustic beam at z = 10 mm; 320 kHz.

Using the same scan data, the Polytec scanning vibrometer software was used to put a narrowband filter around 640 kHz, the second harmonic of 320 kHz (shown in Figure 41). The circular artefacts were again visible showing evidence of strong non-linearity in these regions on the surface of the transducer. The rest of the transducer response at this frequency was not visible, indicating the linearity of the rest of the device.

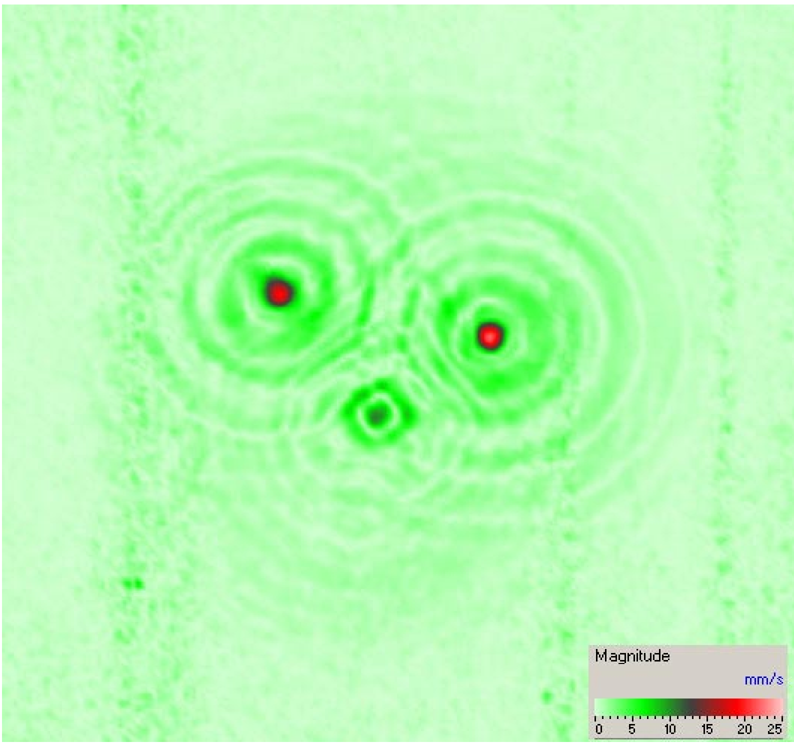

Figure 41. Magnitude (in mm/s) of acoustic beam at z = 10 mm; 640 kHz.

The third harmonic shown in Figure 42 demonstrates the extent of local non-linearity; the circular artefacts are probably caused by defects below the surface of the transducer, believed to be air bubbles inside the transducer face (between the PZT and front face matching layer), which are not visible when the transducer surface is viewed with the naked eye. The circular ripples observed centred around the artefacts may be caused by waves radiating spherically from the artefacts being detected as they impinge on the pellicle. Also visible in Figure 42, are three vertical lines running the length of the scan. These lines were not acoustic properties of the transducer, but rather artefacts of the pellicle, which was hung in the water and was slightly convoluted giving curtain-like ripples to the pellicle. The ripples in the pellicle caused the returning beam of the scanning vibrometer to be scattered away from the vibrometer head, this bad optical return caused the vertical lines to appear on the scan.

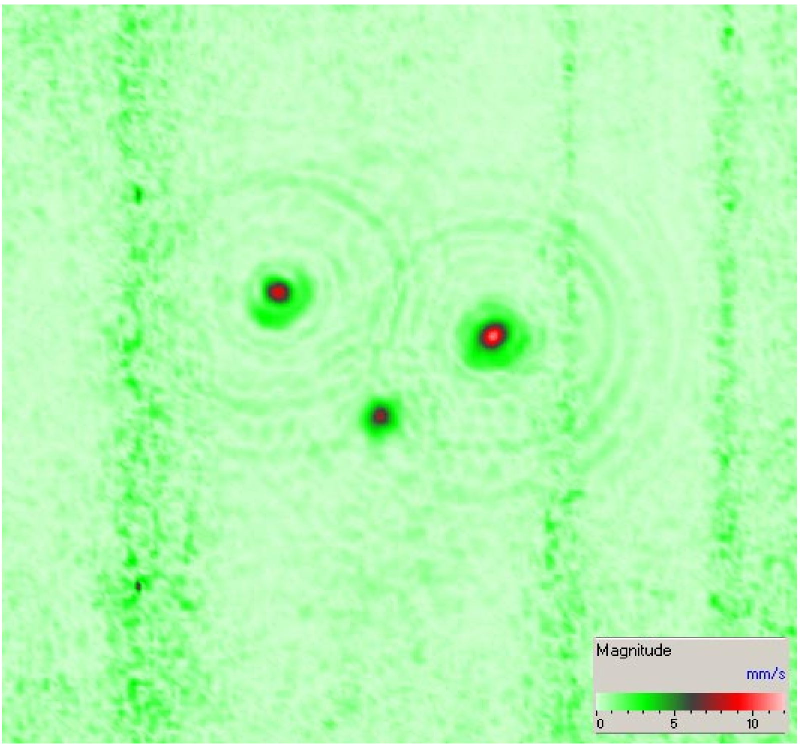

Figure 42. Magnitude (in mm/s) of acoustic beam at z = 10 mm; 960 kHz.

Scans in Figures 40 to 42 show the scanning vibrometers ability to make acoustic near field measurements using a pellicle hung in front of the transducer. It was also possible to use the scanning vibrometer to scan the face of the transducer directly, producing a scan of surface vibrations on the transducer face. The scan area of the surface scan (Figure 43) was set to the shape of the transducer face, giving a circular scan area with a diameter of approximately 150 mm with 10630 scan points. In Figure 43, the scan has been superimposed on to a picture of the transducer taken by the vibrometer head, as described in section 2.4. The circular defects seen in the pellicle near field scans were again visible in this surface scan, other apparent defects on the scan such as the vertical line running the length of the scan to the left of the centre were not believed to be properties of the transducer, but due to the poor reflectivity of the transducer face in that area. The scanning vibrometer had difficulty receiving a return signal from the suspect areas, indicating that these artefacts were non-acoustic. The scanning of a transducer face directly (Figure 43) is a useful diagnostic tool as there is no need to back-propagate a near field scan on to the transducer face, a technique which is prone to errors from the effect of evanescent waves which are difficult to account for if the position of the transducers radiating face is not known exactly.

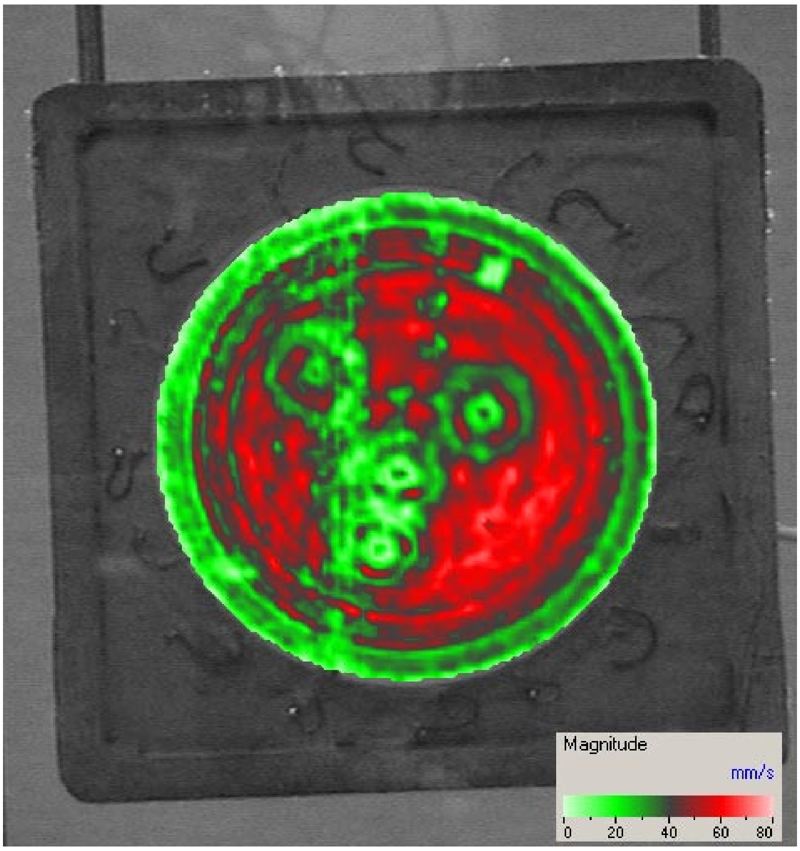

Figure 43. Magnitude (in mm/s) of acoustic beam on transducer surface, 320 kHz.

4.2.2 Hydrophone scans

Measurement scans in the acoustic near field were carried out on the same transducer as described in section 4.2, but using a hydrophone instead of the scanning vibrometer described in section 4.2.1.

The near-field measurements were undertaken by scanning a Reson TC4035 hydrophone over a measurement surface in the acoustic near field and the amplitude of the signal was measured at discrete points. The scans were performed in an automated manner using the positioning systems on the NPL small open tank. The scan (Figure 44) was measured at 10 mm from the transducer face in 2 mm steps over an area of ±100 mm. The transducer was driven at 320 kHz and the signal was time windowed to isolate acoustic reflections, each measurement was then made on the steady state portion of the direct signal.

The hydrophone scan shows the same circular defects visible in the optical scans, the orientation of these artefacts appear to be different to that of the optical scans, this is due to the transducer being mounted upside down (rotated 180°) compared to the optical scans. The plot is also presented as if looking away from the transducer as opposed to the optical scans that look toward the device, accounting for the difference in orientation of the plot.

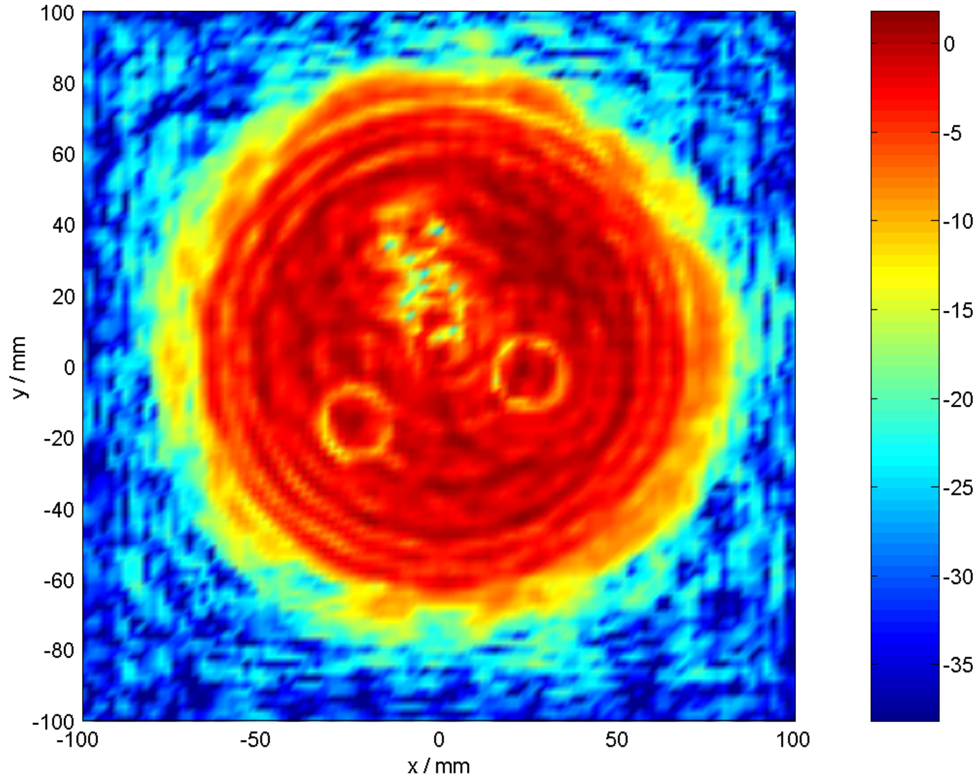

Figure 44. Amplitude (in dB) of back propagated beam at z = 10mm; 320kHz.

4.2.3 Discussion

The results presented demonstrate that optical methods offer potential alternative methods to hydrophone scanning for near field measurements.

The limitations with near field hydrophone scans include:

- The time taken for each hydrophone scan, the scan shown in figure 44 took 12 hours to complete with a resolution of just 2 mm. A similar quality optical scan could be performed in just a few hours.

- The limit to the resolution of a hydrophone scan is set by the size of the hydrophones active element.

- If the hydrophone is not omnidirectional at the frequency of measurement its directional response may have to be taken into account.

- The hydrophone has the problem of disturbing the acoustic field it is interrogating.

To reduce the time of hydrophone scans it is possible to use an array of hydrophones to perform scans but this method has the added problems of greater acoustic disturbance, and the need for the hydrophones within the array to be accurately positioned and well matched in magnitude and phase (or the response of each device to be known).

Optical scan methods have the advantages:

- Potentially more rapid than hydrophone scans.
- The focusing properties of the optic beam allows for potentially high spatial resolution.
- The optic beam is non-perturbing to the acoustic field.

However, potential disadvantages are:

- Flat reflective membrane needed (or reflective transducer surface).
- Optical techniques generally only respond to the out-of-plane component and are therefore directional.
- A tank window is required for optical access (or some other means of delivery).
- Sometimes difficult to interpret signals obtained due to complex acousto-optic interaction.

This last point is particularly important since any acoustic field components travelling in directions that are not parallel to the optical beam may give rise to signals due to refractive index changes (acousto-optic interaction). Such waves will be present in the acoustic near field, and it is difficult to separate these acousto-optic signals from the signals due to the vibration of the transducer surface (or pellicle). In addition, where the acoustic field is non-linear (as would be the case for the parametric array transducer described here when in use), the nature of the acousto-optic effect is not fully understood.

For the reasons stated above, although the potential is clear, further work is required before optical methods can be used reliably for near field scans.

5 OPTICAL FIELD MAPPING STUDY

5.1 Acousto-optic effect

Local density variation in a fluid induced by the passage of an acoustic wave give rise to local perturbations in the refractive index. This acousto-optic effect can be utilised in a number of ways to perform optical measurements of the acoustic field. Previous work at LU used the acousto-optic effect to perform non-invasive measurement of acoustic pressure using interferometric measurement techniques [13] [15] [16] [17]. If the optical beam is allowed to enter a water tank, traverse the acoustic field and reflect back through the acoustic field from a mirror external to the tank, the interferometer will respond to the change in path length or the rate of change in path length. For a vibrometer the local perturbations in the refractive index cause a periodic rate of change of path length which is interpreted as a velocity by the vibrometer. For a physical optical path length, *L*, traversing an acoustic field of width , *Z*, the rate of change of optical path length or modulation of the optical beam can be given by [15];

$$\frac{\mathrm{d}L}{\mathrm{d}t} = \frac{\mathrm{d}\left(2\int_0^z n(z,t)\,\mathrm{d}z\right)}{\mathrm{d}t}, \tag{1}$$

where $n(z,t)$ is the refractive index at a given position, *z*, along the line of integration at given instance in time, *t*. The refractive index change can be related to the pressure by [15];

$$n(z,t) = \left(\frac{\partial n}{\partial P}\right)_S P(z,t), \tag{2}$$

where $P(z,t)$ is the acoustic pressure at a given position, *z*, along the line of integration at a given instance in time, *t*.

5.2 Acousto-optic field mapping using scanning vibrometry

An initial study was undertaken using the Polytec PSV300 scanning vibrometer to investigate the potential of using the acousto-optic effect for acoustic field mapping. The measurement procedure was to align the vibrometer such that the laser beam passed through the glass water tank, measuring 0.3 m by 0.3 m by 1.2 m, and reflected from a stationary mirror positioned externally on the opposite side of the tank as shown in Figure 45. The acoustic projector was then placed in the tank such that the acoustic beam crossed the optical scanning area. A 30 mm piston transducer was used as the projector and was driven with a range of tones using a HP 8111A function generator. The PSV scanning software was used to re-construct the scan image and were displayed in terms of the rate of path length change or velocity experienced by the vibrometer as a result of the acousto-optic effect. The velocities displayed by the vibrometer were arbitrary values related to the acoustic pressure via equations (1) and (2).

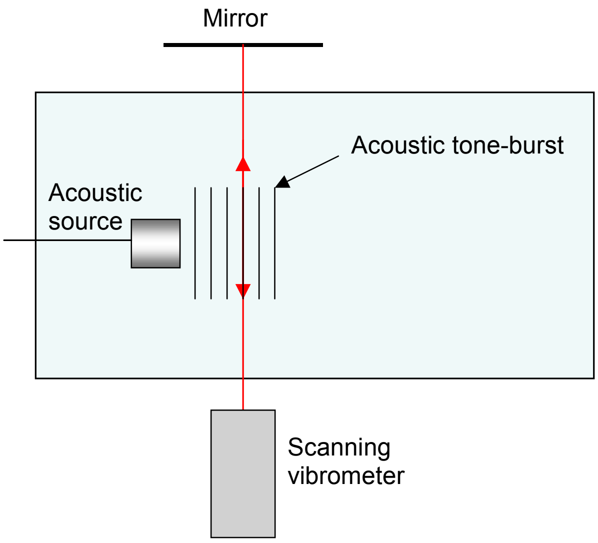

Figure 45. Measurement arrange for scan the acousto-optic region.

The vibrometer results obtained from the 400 kHz and 600 kHz excitation of the 30 mm plane-piston transducer are shown in Figures 46a and 46b respectively. The plots show the camera image with the scan data overlaid, as explained in section 2.4, there is a small lateral offset in the camera and data image due to the physical offset of the axis of the camera lens and that of the optical beam. Although showing the effective rate-of-change of path length, the plots do clearly show the expected behaviour of the piston transducer with a narrow region of higher amplitude produced along the line of propagation and much weaker diffractive components produced laterally from the transducer face. The colour scale employed by the PSV software uses a non-proportional green-red scale, weighted to highlight the peak negative and positive velocities respectively, as can be seen in Figure 46.

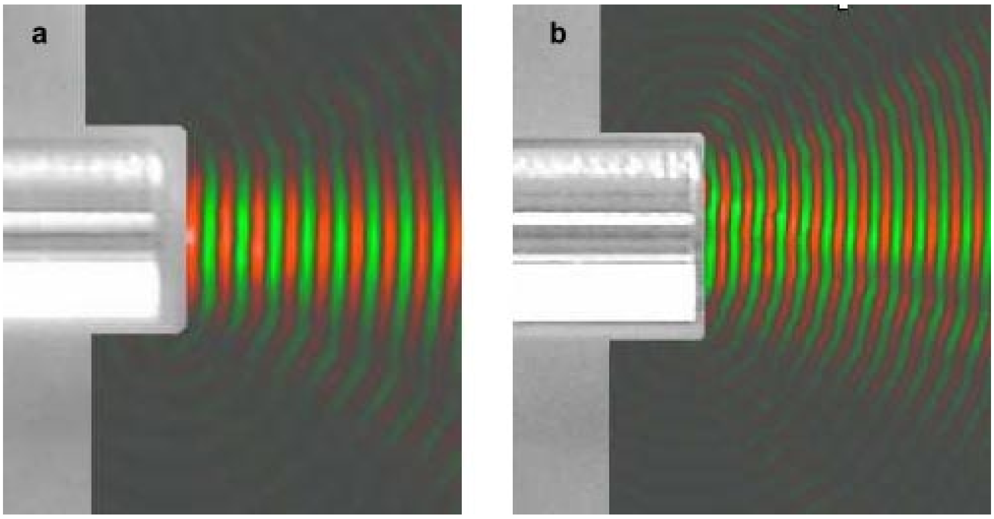

Figure 46. a) 400 kHz tone. b) 600 kHz tone, where green and red represent the negative and positive instantaneous velocity output from the vibrometer.

In addition to the mapping of transducer fields, scans were performed with scattering objects in the acoustic field. One example of this was the insertion of a glass sheet into a 500 kHz acoustic field. The interaction region was scanned as shown in figure 47 to produce an instantaneous velocity plot as shown in Figure 48. The incident acoustic field can be seen in Figure 48 propagating from the top left before reflection from the glass sheet at which point interference occurs with the incident acoustic field. A small amount of transmission can also be seen on the right of the glass sheet.

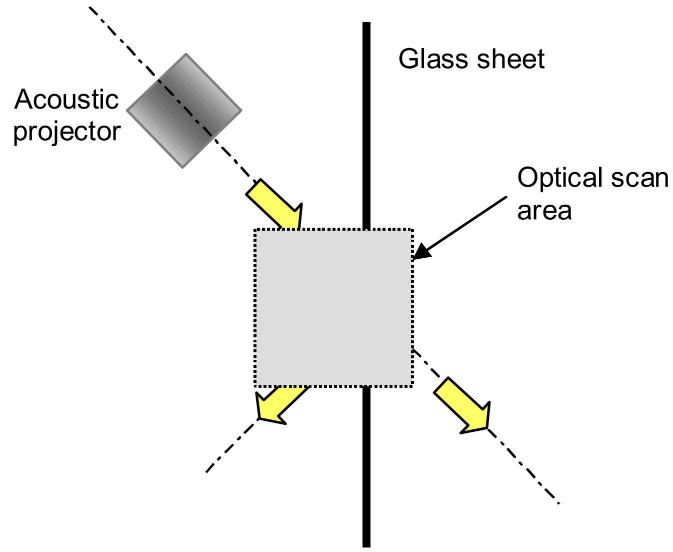

Figure 47. Measurement setup for scanning of scattering field from glass sheet.

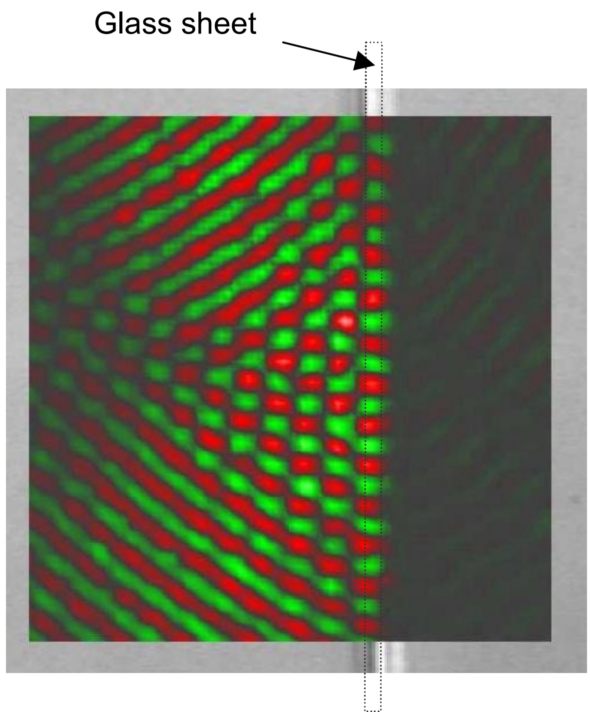

Figure 48. Acousto-optic image from vibrometer for a glass sheet in a 500 kHz acoustic field.

The ultimate aim of the work was to perform measurements using the acousto-optic effect in a lithotripter field, a system used for destroying kidney stones in hospitals and which generate very high acoustic pressures (>100 Mpa). However, the signal processing options on the vibrometer did not allow sufficient dynamic range for the high-pressure field. To overcome this, initial measurements were performed using a small scattering rod (2 mm diameter), scanned across the acoustic field, to reflect a small proportion of the acoustic field energy for measurement by the vibrometer. This work is now continuing with the Hangzhou Applied Acoustics Research Institute (HAARI), China and will be published in the near future. In general, a vibrometer with a greater dynamic range and broader frequency range would be required to capture the resultant harmonics from a high intensity field. It should be noted that although the dynamic range of a standard commercial vibrometer is extremely large, this is usually limited to low 'vibrational' frequency ranges.

5.3 Discussion

The acousto-optic study performed as part of Phase Three of the project has demonstrated that it is possible to characterise acoustic fields in a rapid and non-perturbing way, with resolutions that exceed those possible with conventional hydrophone scans. In addition, the technique offers the considerable potential for use in measuring the highly focussed and highly non-linear fields encountered in lithotripsy and high intensity focussed ultrasonic (HIFU) applications of ultrasound. In such applications, traditional hydrophone sensors can be damaged by the intense acoustic fields, and always perturb the field by their presence. A non-perturbing optical technique would offer significant advantages.

However, work is required to further develop the capability for determining two-dimensional and three-dimensional acoustic field distributions by optical methods. Significant benefits may also be gained from tomographic reconstruction [18] [19] methods, for example for scanning in front of a planar transducer. A better understanding is required of the acousto-optic interaction, particularly where mapping of highly focussed or non-linear fields is required.

The work undertaken as part of this study and previous work by Loughborough University [15] indicate that the acousto-optic interaction has great potential for acoustic mapping applications with several advantages over conventional hydrophone technique and the ability to operate where delicate hydrophone might be damaged.

6 CONCLUSIONS

Initial findings from both Phase One and Two of the project showed the heterodyne interferometer to be the most suitable optical measurement method for this project. The proposed method of measurement was to measure optically the target velocity of a thin membrane in the acoustic field. The main reasons for choosing the heterodyne interferometer configuration are its ability to measure linearly over displacements greater than an optical wavelength, its inherent robustness to external vibration, its direct measurement of target velocity and its relative insensitivity to returning light level. The all-fibre heterodyne interferometer design, proposed in Phase One of this project has now been developed to a first prototype specification and has been extensively tested as part of Phase Two and Three of the project.

In parallel to this development work, several areas of activity have taken place investigating the use of a strip pellicle for optical calibration of hydrophones, optical scanning vibrometry for characterisation of underwater transducers and acoustic field mapping using the acousto-optic scanning techniques.

Measurements performed to assess the suitability of using a narrow strip membrane and a 1.3 m aluminium support frame as a pellicle for optical measurement of acoustic velocity were very successful between 2 kHz and 300 kHz. The agreement between these optical measurements using a Polytec CLV-1000 vibrometer and those performed using a set of reference hydrophones was not worse than 1 dB and predominantly better than 0.5 dB. Higher frequency measurements were performed using a 1 MHz Polytec PSV-300 scanning vibrometer. Although these higher frequency measurements demonstrated the ability to perform optical velocity measurements up to 600 kHz using the a narrow pellicle, the optical measurements showed an overall offset which was thought to be caused by an inaccurate calibration factor above 300 kHz on the vibrometer.

The measurements using the strip pellicle initially introduced some unknown velocity variations with frequency. Further measurements demonstrated that the effect was related to the width of the pellicle and therefore suggested a vibrational membrane mode. Optical performed using Polytec PSV-300 scanning vibrometer clearly demonstrated the existence of modes. The measurements showed that a 1 mm wide reflective pellicle, 1.3 m in length would be sufficient for acoustic measurements up to 600 kHz. The comparison measurements demonstrated the dynamic range of the interferometer, with accurate measurement of velocity up to 5 mm/s, the upper range specified in the project. The lowest velocity measured, with 40 time averages was 0.5 mm/s.

Following the improvements made to the all-fibre heterodyne interferometer in Phase Three of the project, the interferometer was tested at NPL using the small open water tank and narrow strip pellicle arrangement proven with the Polytec. Comparison with a reference hydrophone showed encouraging agreement of around 0.5 dB between 95 kHz and 270 kHz. Outside of this range, the disagreement was worse, particularly at higher frequencies were the disagreement increased with frequency to around 7 dB at 500 kHz. It was thought that this was related to the limitation of the PLL and the use of a 1.5 MHz carrier frequency. It is planned to re-develop the PLL stage of the interferometer to utilise a higher carrier frequency and thus increase the high frequency operation of the interferometer. Measurement of the interferometer noise floor indicated a noise equivalent velocity of around -42 dB re 1 mm/s/Hz$^{1/2}$. It is planned to improve this during Phase Four of the project by optimisation of the electronics and Doppler decoding, and also by increasing the overall light level though the system.

Optical scanning technique were also used for the near field characterisation of a transducer that normally makes up part of a high power parametric array. Optical scanning vibrometry was used to scan both the surface of the transducer and to scan a reflective membrane 10 mm from the face of the transducer. The results were compared similarly with identical scans performed with a hydrophone. Both indicated the presence of circular artefacts in the near field caused by transducer defects. These were much clearer using the optical method due to the greater resolution of the scans. Frequency analysis of the optical results allowed the defects to be identified as non-linear, due to the presence second and third harmonics.

An initial study into the use of the acousto-optic interaction was undertaken to assess the suitability for field mapping of high intensity fields. The results presented show the mapping of standard type transducer fields and scattered acoustic fields. The optical technique provides rapid, non-perturbing, high-resolution maps that would not be achievable with conventional hydrophones. The use of optical techniques is particularly advantages in high intensity focussed ultrasonic (HIFU) and lithotripsy applications where the high intensity field generator can damage or destroy conventional hydrophones.

7 ACKNOWLEDGEMENTS

We gratefully acknowledge the financial support of the UK Department of Trade & Industry (National Measurement System Directorate).

8 REFERENCES

[1] P. D. Theobald, R. C. Preston, S. P. Robinson, R. G. Barham, J. Tyrer, C. Greater, M. Campbell, T. Schlicke, S. Hargrave, C. Swift and R. Crickmore, *Fundamental standards for acoustics based on optical methods – First stage report*, CMAM 83, 2002.

[2] P. D. Theobald, S. P. Robinson, A. D. Thompson, R. C. Preston, P. Lepper, W. Yuebing, C. Swift and J. Tyrer, *Fundamental standards for acoustics based on optical methods – Phase two report for sound in water*, CAIR 3, 2002.

[3] C. B. Scuby and L. E. Drain, *Laser ultrasonics*. Bristol: Adam Hilger, 1990.

[4] D. R. Bacon, *Primary calibration of ultrasonic hydrophones using optical interferometry*, IEEE Transactions on Ultrasonics, Ferroelectrics, and Frequency Control, Vol. 35, No. 2, pp. 152-161, 1988.

[5] D.R. Bacon, *The improvement and evaluation of a laser interferometer for the absolute measurement of ultrasonic displacements in the frequency range up to 15 MHz*. NPL Acoustics Report Ac109. November 1986.

[6] C. Koch and W. Molkenstruck, *Primary calibration of hydrophones with extended frequency range 1 to 70 MHz using optical interferometry*, IEEE Transactions on Ultrasonics, Ferroelectrics, and Frequency Control, Vol. 46, No. 5, pp. 1303-1314, 1999.

[7] D. R. Bacon, R. C. Chivers and J. N. Som, *The acousto-optic interaction in the interferometric measurement of ultrasonic transducer surface motion*, Ultrasonics, Vol. 31, No. 5, pp. 321-325, 1993.

[8] T. J. Esward and S. P. Robinson, *Extending the frequency range of the National Physical Laboratory primary standard laser interferometer for hydrophone calibrations to 60 MHz*, IEEE Transactions on Ultrasonics, Ferroelectrics, and Frequency Control, Vol. 46, No. 3, pp. 737-744, 1999.

[9] R. C. Preston, S. P. Robinson, B. Zeqiri, T. J. Esward, P. N. Gelat and N. D. Lee, *Primary calibration of membrane hydrophones in the frequency range 0.5 MHz to 60 MHz*, Metrologia, Vol. 36, pp. 331-343, 1999.

[10] W. Yuebing and H. Yongjun, *The application of optical interferometry in the measurement of hydrophones*, Proceedings of the Institute of Acoustics, Calibration and measurement in underwater acoustics, Volume25, Part 1, 2003.

[11] P. D. Theobald, C. J.Bickley and S. P. Robinson, Recent progress at NPL in the use of optical techniques for hydrophone calibration, Proceedings of the Institute of Acoustics, Calibration and measurement in underwater acoustics, Volume25, Part 1, 2003.

[12] A. R. Harland, *The application of laser Doppler velocimetry to the measurement of underwater acoustic pressure fields*, PhD thesis submitted to Loughborough University, 2002.

[13] A. R. Harland, J. N. Petzing and J. R. Tyrer, *Non-invasive measurements of underwater pressure fields using laser Doppler velocimetry*, Journal of Sound and Vibration, Vol. 252, No. 1, pp. 169-177, 2002.

[14] *Fourier Acoustics: Sound radiation and nearfield holography*, Ed. G Williams, Academic Press, 1999.

[15] A. R. Harland, J. N. Petzing, C. Bickley, S. P. Robinson, J. R. Tyrer and R. C. Preston, Application and assessment of laser Doppler velocimetry for underwater acoustic measurements, Journal of Sound and Vibration, accepted for publication, 2002.

[16] A. R. Harland, The application of laser Doppler velocimetry to the measurement of underwater acoustic pressure fields, PhD submitted for examination to Loughborough University, 2002.

[17] A. R. Harland, J. N. Petzing and J. R. Tyrer, *Non-invasive measurements of underwater pressure fields using laser Doppler velocimetry*, Journal of Sound and Vibration, Vol. 252, No. 1, pp. 169-177, 2002.

[18] R. Reibold and P. Kwiek, *Uncertainty considerations of ultrasonic field mapping by light-diffraction tomography*, Ultrasonics, Vol. 35, pp. 187-193, 1997.

[19] T. A. Pitts and J. F. Greenleaf, *Three-dimensional optical measurement of instantaneous pressure*, J. Acoust. Soc. Am., Vol. 108, No. 6, pp. 2873-2883, 2000.